UNIVERSIDADE FEDERAL DO CEARÁ

CENTRO DE TECNOLOGIA

DEPARTAMENTO DE ENGENHARIA DE TELEINFORMÁTICA

PROGRAMA DE PÓS-GRADUAÇÃO EM ENGENHARIA DE TELEINFORMÁTICA

CARLOS IGOR RAMOS BANDEIRA

INTERFERENCE ALIGNMENT IN WIRELESS COMMUNICATION SYSTEMS: PRECODING DESIGN, SCHEDULING AND CHANNEL IMPERFECTIONS

FORTALEZA

2012

CARLOS IGOR RAMOS BANDEIRA

INTERFERENCE ALIGNMENT IN WIRELESS COMMUNICATION SYSTEMS: PRECODING DESIGN, SCHEDULING AND CHANNEL IMPERFECTIONS

Dissertação submetida à coordenação do Programa de Pós-Graduação em Engenharia de Teleinformática, da Universidade Federal do Ceará, como requisito parcial para a obtenção do grau de Mestre em Engenharia de Teleinformática. Área de Concentração: Sinais e Sistemas.

Orientador: Prof. Dr. Walter da Cruz Freitas Júnior

FORTALEZA
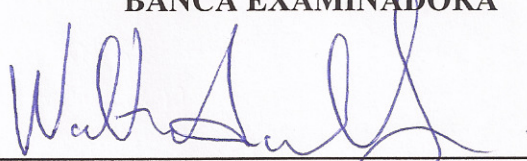**2012**

CARLOS IGOR RAMOS BANDEIRA

INTERFERENCE ALIGNMENT IN WIRELESS COMMUNICATION SYSTEMS: PRECODING DESIGN, SCHEDULING AND CHANNEL IMPERFECTIONS

Dissertação submetida à Coordenação do Programa de Pós-Graduação em Engenharia de Teleinformática, da Universidade Federal do Ceará, como requisito parcial para a obtenção do grau de Mestre em Engenharia de Teleinformática.
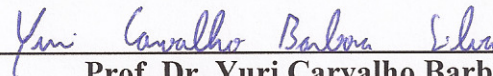Área de concentração: Sinais e Sistemas

Aprovada em 29/06/2012.
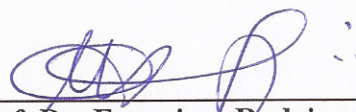
BANCA EXAMINADORA

Prof. Dr. Walter da Cruz Freitas Júnior (Orientador)
Universidade Federal do Ceará - UFC

Prof. Dr. Yuri Carvalho Barbosa
Universidade Federal do Ceará - UFC

Prof. Dr. Francisco Rodrigo Porto Cavalcanti
Universidade Federal do Ceará - UFC

Prof. Dr. Richard Demo Souza
Universidade Tecnológica Federal do Paraná - UTFPR

Dedicatories

Dedico este trabalho com muito carinho, aos meus pais, Carlos e Ozanira, que são meus maiores incentivadores, às minhas irmãs Karla e Carolina, as quais sou imensamente grato por serem minhas fiéis companheiras em todos os momentos, e ao meu sobrinho Samuel Bruno, o qual me ensina todos os dias que ser feliz é simples.

Acknowledgements

First and foremost, I would like to thank God for giving me the life and for always guiding me through hard, but safe ways whose goal is strengthen us. I would also like to thank my family, specially my mother Ozanira, as well as my sisters and my nephew for their love, comprehension and support through all my life. I also thank my girlfriend Gabriela for her help always I need.

I would like to thank Professor Walter, Professor Yuri and Professor Rodrigo for believing me and for giving me the opportunity to work at GTEL. I would also like to thank all UFC.32 team for their guidance and technical support in my research. I am also grateful to friends and colleagues from GTEL, whose suggestions and encouragement were invaluable throughout my Master's course.

Thanks very much!!!
Carlos Igor.

"A tarefa não é tanto ver aquilo que ninguém viu, mas pensar o que ninguém ainda pensou sobre aquilo que todo mundo vê."

Arthur Schopenhauer

Abstract

In multiuser MIMO systems, the transmitter can select a subset of antennas and/or users which have good channel conditions to maximize the system throughput using various selection criteria. Furthermore, precoding can provide free interference dimensions. The Interference Alignment (IA) is based on the concept of precoding and it offers different trade-offs between complexity and performance. The basic idea of Interference Alignment consists in precoding the transmitted signals such that they are aligned at the receiver where they constitute interference, while at the same time disjointed from the desired signal. However, the Channel State Information (CSI) has been a concern because it impacts the performance of IA algorithms. Hence, we propose to analyze the performance of antenna selection and multiuser diversity together in order to allow opportunistic IA using several criteria over the disturbance of CSI. Analyses and simulations verify the behavior of the proposed scheme.

Keywords: Interference Alignment, Precoding, Antenna Selection, Opportunistic User Selection, MIMO Interfering Broadcast Channels.

Resumo

Em sistemas MIMO multiusuário, o transmissor pode selecionar um subconjunto de antenas e/ou usuários que têm bons canais para maximizar o rendimento do sistema usando vários critérios de seleção. Além disso, os pré-codificadores podem proporcionar dimensões livres de interferência. O alinhamento de interferência (IA) é baseado no conceito de pré-codificação e oferece diferentes compromissos entre complexidade e desempenho. A idéia básica do Alinhamento Interferência consiste em pré-codificar os sinais transmitidos de maneira que os mesmos sejam alinhados no receptor, em que eles constituem interferência, enquanto que ao mesmo tempo os separa do sinal desejado. No entanto, a Informação do Estado do Canal (CSI) tem sido uma preocupação para os pesquisadores porque ela tem um impacto no desempenho de algoritmos de IA. Assim, nos propomos a analisar o desempenho da seleção de antena e diversidade multiusuário em conjunto, a fim de permitir o IA oportunista usando vários critérios com relação à perturbação da CSI. Análises e simulações verificam o comportamento do esquema proposto.

Palavras-Chave: Alinhamento de Interferência, Pré-codificação, Seleção de Antenas, Seleção de Usuários Oportunística, Canais MIMO Interferentes.

List of Figures

List of Tables

List of Algorithms

List of Acronyms

BER   Bit Error Rate

BS   Base Station

CDF   Cumulative Distribution Function

CSI   Channel State Information

DoF   Degrees of Freedom

DPC   Dirty Paper Coding

D2D   Device-to-Device

IA   Interference Alignment

IC   Interference Channel

KKT   Karush-Kuhn-Tucker

MIMO-IC MIMO Interference Channel

MIMO-X MIMO-X

MIMO   Multiple Input Multiple Output

MMSE   Minimum Mean Square Error

PSD   Positive Semidefinite

PSK   Phase-Shift Keying

SINR   Signal-to-Interference-plus-Noise Ratio

SISO   Single-Input Single-Output

SNR   Signal-to-Noise Ratio

SVD   Singular Value Decomposition

ZF   Zero-Forcing

Contents

Chapter 1

Introduction

It is well known that the capacity of the single user point-to-point Multiple Input Multiple Output (MIMO) channels, with M transmit antennas and N receive antennas, increases linearly with $\min(M, N)$ in the high Signal-to-Noise Ratio (SNR) regime [1, 2]. This linear growth, addressed as Degrees of Freedom (DoF) or *capacity pre-log factor* is commonly known, in the single user systems, as *multiplexing gain*, which is defined as

$$\eta \triangleq \lim_{\rho \to \infty} \frac{C(\rho)}{\log(\rho)},$$
(1.1)

where ρ represents the SNR.

Similarly, in the multiuser case, it is useful to characterize the DoF of the network (related to the sum rate capacity of the network). To give it a simple intuition, it is worth to note that:

i. The degrees of freedom of a network may be interpreted as the number of resolvable (interference-free) signal space dimensions and its determination can be considered as a preliminary characterization of the capacity for a network;

ii. It provides a good capacity approximation in the high SNR regime.

In practice, the interference present in a system is usually handled by *interference avoidance*, according to which users coordinate their transmissions by orthogonalizing the signals in the time or frequency domains, or by *treating-interference-as-noise*, according to which users increase their respective transmission power, treating each interference as noise [3]. The characterization of obstruction, that interference imposes on the capacity, is not an easy task. For instance the capacity

of the two-user Gaussian interference channel (with single antennas) was considered an open problem for 30 years until 2008 when Tse *et al.* [4] derived the capacity for such systems. Unfortunately, the Interference Channel (IC) capacity region is still unknown in general, but in the last five years, recent studies have provided the multiplexing gain characterization of interference networks. Several new techniques have been discovered and among them there is one known as *Interference Alignment (IA)*. It has been presented in [5] as a key approach for the exploitation of the DoF.

In the next section, we present the basic idea about interference alignment and a general overview highlighting several approaches and motivations in the literature.

1.1 Overview and Motivation

The basic idea of interference alignment is to align the signal spaces at receivers where they constitute the interference while in the desired receivers they are separable [6]. In other words, IA refers to the consolidation of multiple interfering signals into a small subspace at each receiver so that the number of interference-free dimensions remaining for the desired signal can be maximized [7]. The optimality of these schemes at high SNR is interesting, because they treat all interference as noise and require no multiuser detection [8], such that a simple Zero-Forcing (ZF) filter is enough to cancel the interference (which spans only one dimension).

The application of interference alignment is very general, in the sense that the signals can be aligned in any dimension, including time, frequency, or space. It can be viewed as a cooperative approach because the transmitters may neglect the performance of their own link allowing that other users cancel interference perfectly [9]. A less altruistic proposal can be employed when each user does not seek to align completely the interference caused at the non-intended receivers, but only minimize it as well as maximizing the user's own Signal-to-Interference-plus-Noise Ratio (SINR), for instance.

Two main issues faced by interference alignment schemes are:

i. The number of alignment constraints grows very rapidly when the number of interfering users is increased. For instance, in a K-user interference channel, each of the K receivers needs an alignment

of $K - 1$ interfering signal spaces, for a total of $O(K^2)$ signal space alignment constraints. Since there are only K signal spaces (one at each transmitter) to be chosen in order to satisfy $O(K^2)$ signal space alignment constraints, the problem can quickly appear infeasible.

ii. The diversity of channels which enables the relativity of alignment is often a limiting factor.

Further issues to be dealt by interference alignment schemes include the imperfect, noisy, localized and possibly delayed nature of channel knowledge feedback to the transmitters where such knowledge is crucial to achieve interference alignment [10].

There are two versions of interference alignment in the literature: *signal space alignment* and *signal scale alignment.* The interference alignment in signal vector space was initially introduced by Maddah-ali *et al.* (2006) [11], whose iterative schemes were formulated for optimizing transmitters and receivers jointly with dirty paper coding and successive decoding schemes. Signal space alignment approaches are applicable to interference channels with time varying/frequency selective channel coefficients. Signal scale alignment schemes, on the other hand, use structured coding, e.g. lattice codes, to align interference in the signal level and are especially useful in the case of constant channels [3]. Most of the literature so far focuses on signal space alignment and we follow them.

Signal space interference alignment was introduced for the K-user interference channel with equal number of antennas at all transmitters and receivers by Cadambe and Jafar (2008) [12], and later extended to the unequal number of antennas by Gou and Jafar (2008) [13]. Similarly, interference alignment schemes were proposed for X networks[1] with arbitrary number of users by Cadambe and Jafar (2008) [14]. In addition, cellular networks were considered by Suh and Tse (2008) [15] and by Sun, Liu, and Zhu (2010) [16].

Schemes for signal space alignment are attractive due to the analytical tractability as well as the useful insights offered to finite SNR regimes, where they may be naturally combined with selfish approaches [17]. Within the class of signal vector space interference alignment schemes, the alignment in spatial dimension through multiple antennas (MIMO)

---

[1]In X networks useful signal is also transmitted in the crossed links.

is found to be more robust to practical limitations such as frequency offsets than alignment in time or frequency dimensions [18]. However, the feasibility of linear interference alignment for general MIMO interference networks remains an open problem [8].

Additionally, for low to moderate SNRs the complete alignment does not generally maximize the sum utility and there is interest in finding precoders that relax the perfect alignment constraint with the objective of obtaining a better sum rate performance [9]. That is, each transmitter will face a trade-off between finding a precoder that minimizes the interference that its own receiver sees ("help yourself" approach) and minimizing the interference that it causes at the non-intended receivers ("do no harm" approach). In [19] the idea of interference price was proposed where each transmitter's beams were treated separately and associated with an interference price, which corresponds to a metric of how much the utility will decrease per marginal increase in interference after the appropriate receive filter is applied. This creates a link between the egoistic and altruistic approaches.

In [20] game-theoretic concepts are explored to propose a beamforming design framework which explicitly addressed the compromise between the beamforming gain at the receiver (Egoism) and the mitigation of the interference created at other receivers (Altruism). The Egoism versus Altruism balancing parameter in the distributed beamforming algorithm proposed in [20] can be shown to coincide with the pricing parameters proposed in [19].

In the literature two strategies employ additional DoF to improve diversity: antenna selection and multiuser diversity. A combination of IA and antenna selection techniques using several metrics to determine the most appropriate measure is presented In [21] while an opportunistic user selection in a limited feedback environment is presented in [22].

Other approaches as blind and retrospective interference alignment are introduced respectively in [23] and [24]. Blind interference alignment is defined as the idea that even if the actual channel coefficient values are entirely unknown to the transmitters, interference alignment may be possible based on the knowledge of the distinct autocorrelation properties of the channels seen by different receivers [10]. On the other hand, retrospective interference alignment refers to interference alignment schemes that exploit only delayed CSIT, which is assumed

independent of the current channel state. The delayed CSIT is useful for the transmitter to the extent that it helps learn the current channel state, but is surprising that it can increase the available DoF.

In general, the application of interference alignment has focused on single hop networks considering the MIMO Y channel [25] while applications of interference alignment to multihop interference networks are still not well understood. Indeed, Cadambe and Jafar showed in [26] that multihop interference networks with relays do not increase the DoF when the network is fully connected, i.e., all channel coefficients are nonzero and global channel knowledge is available, for almost all channel coefficient values. However, they can still be helpful in aiding interference alignment with finite symbol extensions simplifying the achievable scheme [27].

Other channel model approaches are available in the literature regarding the algorithms and strategies for avoiding or mitigating the interference. A particular case of the scenario described in previous works as an option is called partially connected K-user MIMO Interference Channel (MIMO-IC), where each user receives interference only from a limited subset of the K transmitters, and where each transmitter interferes with a limited subset of receivers [28, 29].

Another recent approach is to join femtocells with IA in a given network [30, 31]. In order to manage the uplink interference caused by macrocell users at the femtocell base stations, cooperation between macrocell users with the closest femtocell base stations could be used to align the received signals of macrocell users in the same subspace at multiple femtocell base stations simultaneously.

A promising technique to provide efficient use of available spectrum is to enable wireless direct communication of Device-to-Device (D2D) [32]. In [33] three grouping schemes are proposed for the D2D users where D2D pairs are grouped into three pairs such that IA can be applied using a limited number of signal extensions.

1.2 Outline and Contributions

This master thesis is organized into the following chapters:

Chapter 2: Concepts of Interference Alignment. In this chapter, we cover briefly the notion of DoF, in order to verify the detrimental effect of interference on the DoF. In the literature, some key system

model scenarios are often considered by the researchers. They are described and compared regarding their behavior and upper bound DoF characterization. Finally, we present the preliminary concepts about the IA technique, including a discussion about feasibility conditions and channel knowledge feedback, e.g., correlation and Channel State Information (CSI).

Chapter 3: Closed-Form Solutions and Algorithms for MIMO Interference Alignment Systems. In this chapter, we present the usual closed-form solution for three users in the IC, and introduce some of the algorithms in the literature, which were roughly divided in two categories: centralized and distributed algorithms. A significant contribution is the analysis of a general utility function for the pricing algorithm in relation to the interference price. Moreover, we gather some methods concerning the initialization of the precoding matrices used in the computer simulations.

Chapter 4: Scheduling Strategies. In this chapter, we analyze the use of antenna and user selection schemes in order to improve IA performance and to find an appropriate metric which allows to increase the subspace distance for maximizing the capacity of the system. A significant contribution is the performance evaluation of the Fubini-Study distance [34] being used as metric for antenna and user selection. Moreover, we propose a joint antenna and user selection technique and evaluate its behavior through computer simulations.

Chapter 5: Simulation Results. In this chapter, we present the simulation results of the presented algorithms, considering antenna correlation, variable CSI and external interference besides the limitations of IA.

Chapter 6: Conclusions and Perspectives. In this chapter, we summarize the conclusions and provide some perspectives.

Chapter 2

Concepts of Interference Alignment

The basic idea of Interference Alignment consists in precoding the transmitted signals such that they are aligned at the receiver where they constitute interference, while at the same time, disjointed from the desired signal. Thus, the desired signal and the interference are easily separated at each receiver.

In this chapter we introduce the technical background needed to understand the concept of IA. Section 2.2 presents the system model and investigates other approaches for channel model while Section 2.3 illustrates how the interference alignment works, presenting the main characteristics of this technique and the feasibility conditions. Finally, conclusions are given in Section 2.4.

2.1 Preliminaries

In this section initially we present the notion of DoF, and apply this definition to derive the achievable DoF for a single user MIMO link, and then for a multiuser MIMO link with interference. Furthermore, we mathematically establish the detrimental effect of interference on the DoFs.

2.1.1 Degrees of Freedom

The DoF metric is primarily concerned with the limit where the total transmit power approaches infinity, while the values of channel coefficients and the local noise power remain unchanged. The DoF metric η is defined as

$$\eta \triangleq \lim_{\rho \to \infty} \frac{C(\rho)}{\log(\rho)}, \tag{2.1}$$

where C is the capacity and ρ represents the SNR. It is also equivalently stated as

$$C(\rho) = \eta \log(\rho) + o \log(\rho), \tag{2.2}$$

where the $o \log(\rho)$ term is some function $f(\rho)$ such that

$$\lim_{\rho \to \infty} \frac{f(\rho)}{\log(\rho)} = 0. \tag{2.3}$$

Considering the capacity of a single user $M \times N$ MIMO link with AWGN, the Shannon capacity limit is given by

$$C = \log \left| \mathbf{I}_N + \frac{P}{M\sigma_n^2} \mathbf{H}\mathbf{H}^H \right|, \tag{2.4}$$

where P is total transmit power across all antennas and σ_n^2 the noise variance at the receiver. It can be written as:

$$
\begin{aligned}
C &= \log \left| \mathbf{I}_N + \frac{P}{M\sigma_n^2} \mathbf{H}\mathbf{H}^H \right| \\
&= \log \left| \mathbf{I}_N + \frac{P}{M} (\mathbf{H}\mathbf{H}^H)(\sigma_n^2 \mathbf{I}_N)^{-1} \right| \\
&= \log \left| \mathbf{I}_N + \frac{P}{M} \mathbf{Q}_S (\sigma_n^2 \mathbf{I}_N)^{-1} \right|,
\end{aligned}
\tag{2.5}
$$

where $\mathbf{Q}_S$ is the $N \times N$ desired signal covariance matrix. The Singular Value Decomposition (SVD) can be applied to the Hermitian matrix $\mathbf{Q}_S = \mathbf{U}\mathbf{D}\mathbf{U}^H$, where $\mathbf{U}$ is an $N \times d$ unitary matrix, $d \leq N$ is the rank of the matrix and $\mathbf{D}$ a diagonal $N \times N$ matrix with the d eigenvalues of $\mathbf{Q}_S$ composed by λ_S^i ($1 \leq i \leq d$) on its main diagonal. Thus we can rewrite the capacity as

$$
\begin{aligned}
C &= \log \left| \mathbf{I}_N + \frac{P}{M\sigma_n^2} \mathbf{H}\mathbf{H}^H \right| \\
&= \log \left| \mathbf{I}_N + \frac{P}{M\sigma_n^2} \mathbf{D} \right| \\
&= \sum_{i=1}^{d} \log \left(1 + \frac{P}{M\sigma_n^2} \lambda_S^i \right) \\
&= \sum_{i=1}^{d} \log \left(1 + \rho \lambda_S^i \right).
\end{aligned}
\tag{2.6}
$$

It is convenient to think of the DoF as the number of signaling dimensions in a system (frequency, time, space), where one signal dimension corresponds to one interference-free AWGN channel. For the single user $M \times N$ MIMO link, the DoF is the number of equivalent d-parallel non-interfering AWGN links. Mathematically, they can be defined as:

$$\eta = \lim_{\rho \to \infty} \frac{C(\rho)}{\log(\rho)} = \lim_{\rho \to \infty} \frac{\sum_{i=1}^{d} \log\left(1 + \rho \lambda_S^i\right)}{\log(\rho)}$$

$$\approx \sum_{i=1}^{d} \lim_{\rho \to \infty} \frac{\log(\rho \lambda_S^i)}{\log(\rho)} = d, \tag{2.7}$$

where the last equality follows from the application of L'Hosptial's rule to deduce that $\dfrac{\log(ax)}{\log(x)} = 1$. Thus, in the presence of white noise only, an $M \times N$ MIMO link has d DoF, where d is the rank of the channel matrix.

However, in a multiuser environment, each user is subject to interference from all the remaining transmitters. Therefore, extending the model in (2.5), it can be shown that the capacity of an $M \times N$ MIMO link in the presence of interference is given by

$$C = \log \left| \mathbf{I}_N + \frac{P}{M} \mathbf{Q}_S \mathbf{Q}_{IN}^{-1} \right|, \tag{2.8}$$

where $\mathbf{Q}_{IN}$ is the interference plus noise covariance matrix given by

$$\begin{aligned} \mathbf{Q}_{IN} &= \mathbf{Q}_I + \mathbf{Q}_N \\ &= \mathbf{Q}_I + \sigma_n^2 \mathbf{I}_N \\ &= \rho_I \mathbf{D}_I + \sigma_n^2 \mathbf{I}_N \\ &= \rho^\theta \mathbf{D}_I + \sigma_n^2 \mathbf{I}_N, \end{aligned} \tag{2.9}$$

where $\mathbf{D}_I$ is the diagonal matrix of eigenvalues of the interference matrix, $\rho_I = \rho^\theta$, $\theta \in \mathbb{R}$ and ρ^θ is the power of interference relatively to the desired signal power.

Now, we can write the capacity C as

$$C = \log \left| \mathbf{I}_N + \frac{P}{M} \mathbf{Q}_S \mathbf{Q}_{IN}^{-1} \right| = \log \left| \mathbf{I}_N + \frac{P}{M} \mathbf{D}(\rho^\theta \mathbf{D}_I + \sigma_n^2 \mathbf{I}_N)^{-1} \right|, \tag{2.10}$$

Since all the matrices in the above expression are diagonal, and assuming

without loss of generality that $\mathbf{Q}_S$ and $\mathbf{Q}_{IN}$ have the same rank d, we rewrite the capacity C as

$$C = \log \left| \mathbf{I}_N + \frac{P}{M} \mathbf{D}(\rho^\theta \mathbf{D}_I + \sigma_n^2 \mathbf{I}_N)^{-1} \right| = \sum_{i=1}^{d} \log \left[1 + \frac{\rho \lambda_S^i}{(\rho^\theta \lambda_I^i + \sigma_n^2)} \right], \qquad (2.11)$$

Using Equation (2.1), then

$$\begin{aligned}
\eta &= \lim_{\rho \to \infty} \frac{C(\rho)}{\log(\rho)} = \lim_{\rho \to \infty} \frac{\sum_{i=1}^{d} \log \left[1 + \frac{\rho \lambda_S^i}{(\rho^\theta \lambda_I^i + \sigma_n^2)} \right]}{\log(\rho)} \\
&\approx \sum_{i=1}^{d} \lim_{\rho \to \infty} \frac{\log[\rho^{1-\theta}(\lambda_S^i / \lambda_I^i)]}{\log(\rho)} = \sum_{i=1}^{d} \lim_{\rho \to \infty} \frac{\log(\rho^{1-\theta}) + \log(\lambda_S^i / \lambda_I^i)}{\log(\rho)} \\
&= \sum_{i=1}^{d} \lim_{\rho \to \infty} \frac{\log(\rho^{1-\theta})}{\log(\rho)} = d(1 - \theta), \qquad (2.12)
\end{aligned}$$

when $\rho^\theta \lambda_I^i \gg \sigma_n^2$. Since d is a positive integer, and θ real number, we can deduce the following:

i. $\theta < 1 \Rightarrow \eta > 0$;

ii. $\theta = 1 \Rightarrow \eta = 0$;

iii. $\theta > 1 \Rightarrow \eta < 0$.

Thus, the DoF exists in cases when $\theta < 1$, i.e., the power of interference ρ^θ is less than the power of the desired signal ρ. Conversely, when the power of the interference is equal or greater than the power of the signal ($\theta \geqslant 1$), the DoF collapses and the system becomes interference limited (a negative value for η implies that the capacity decreases with ρ) [35]. This derivation clearly shows the detrimental effect of interference on the DoF.

2.1.2 Possible Scenarios

The concept of interference alignment is very general and can be applied in several different scenarios, where each one yields a slightly different system model. In all models there is a precoding vector (or matrix) to align the interference and a linear receive filter vector (or matrix) to cancel the interference. Hereafter, two key scenarios are described and compared, which are denominated as the MIMO-X channel and the MIMO interference channel.

MIMO-X Channel

The MIMO-X channel is the most generic case when the interference alignment is performed with no symbol extensions, that is, interference is aligned in the space domain. Each transmitter sends different data for each receiver as illustrated in Figure 2.1 for the two-user case. That is, each receiver will see both useful information and interference from each transmitter.
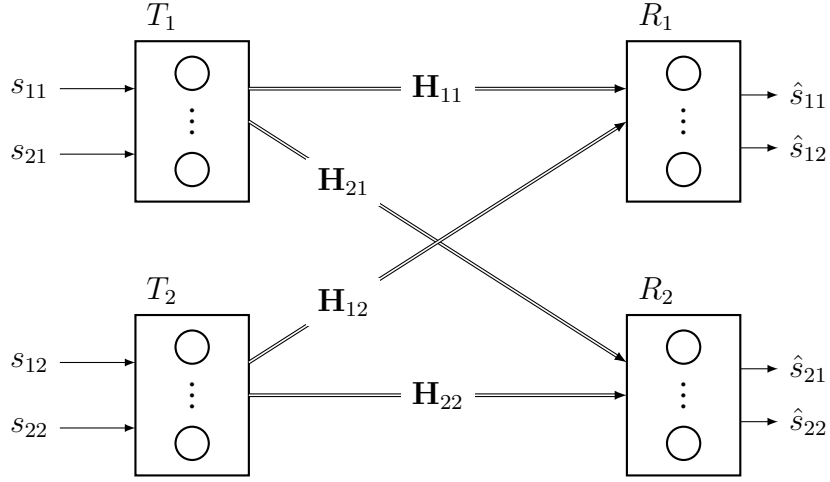
Figure 2.1 – MIMO-X Channel.

In Figure 2.1, the transmitter T_1 and T_2 send transmit data $s_{11}, s_{21}, s_{12}, s_{22}$ for the receivers R_1 and R_2. Each receiver will then apply two different steering vectors, one at a time, in order to recover the two information signals. Then, the received signals $\mathbf{y}_1, \mathbf{y}_2$ (before cancelling the interference) are given by [36]

$$\mathbf{y}_1 = \mathbf{H}_{11}\left(\mathbf{v}_{11}s_{11} + \mathbf{v}_{21}s_{21}\right) + \mathbf{H}_{12}\left(\mathbf{v}_{12}s_{12} + \mathbf{v}_{22}s_{22}\right) + \mathbf{n}_1, \qquad (2.13)$$

$$\mathbf{y}_2 = \mathbf{H}_{21}\left(\mathbf{v}_{11}s_{11} + \mathbf{v}_{21}s_{21}\right) + \mathbf{H}_{22}\left(\mathbf{v}_{12}s_{12} + \mathbf{v}_{22}s_{22}\right) + \mathbf{n}_2, \qquad (2.14)$$

where $\mathbf{v}_{11}, \mathbf{v}_{21}, \mathbf{v}_{12}, \mathbf{v}_{22}$ are the corresponding precoding vectors, and the matrices $\mathbf{H}_{ij}$ contain the MIMO channel coefficients between transmitter j and receiver i.

The transmit signals s_{11}, s_{12} and s_{21}, s_{22} can be recovered by multiplying the received signals $\mathbf{y}_1$ in receiver 1 and $\mathbf{y}_2$ in receiver 2 by the steering vectors $\mathbf{u}_{11}, \mathbf{u}_{12}$ and $\mathbf{u}_{22}, \mathbf{u}_{21}$, respectively. The condition for the (complete) interference alignment and correct signal recovery at both receivers is that the steering vectors need to be in the null space of the corresponding

interference (equivalent channel after the precoding). This is summarized in Equations (2.15)-(2.18) below [36]

$$\text{Interference at Receiver 1} \begin{cases} \mathbf{u}_{11}^H \left[\mathbf{H}_{12}\mathbf{v}_{12} \ \mathbf{H}_{12}\mathbf{v}_{22} \ \mathbf{H}_{11}\mathbf{v}_{21} \right] = \mathbf{0}, & (2.15) \\ \mathbf{u}_{12}^H \left[\mathbf{H}_{11}\mathbf{v}_{11} \ \mathbf{H}_{11}\mathbf{v}_{21} \ \mathbf{H}_{12}\mathbf{v}_{22} \right] = \mathbf{0}, & (2.16) \end{cases}$$

$$\text{Interference at Receiver 2} \begin{cases} \mathbf{u}_{21}^H \left[\mathbf{H}_{22}\mathbf{v}_{12} \ \mathbf{H}_{22}\mathbf{v}_{22} \ \mathbf{H}_{21}\mathbf{v}_{11} \right] = \mathbf{0}, & (2.17) \\ \mathbf{u}_{22}^H \left[\mathbf{H}_{21}\mathbf{v}_{11} \ \mathbf{H}_{21}\mathbf{v}_{21} \ \mathbf{H}_{22}\mathbf{v}_{12} \right] = \mathbf{0}, & (2.18) \end{cases}$$

and in order for these steering vectors to exist it is required that the quantities in brackets do not have a full rank. This can be achieved by using precoding vectors such that $\mathbf{H}_{21}\mathbf{v}_{11} = \mathbf{H}_{22}\mathbf{v}_{12}$ and $\mathbf{H}_{11}\mathbf{v}_{21} = \mathbf{H}_{12}\mathbf{v}_{22}$.

The upper bound DoF of the $M \times N$ user X network scenario ($\eta_{\text{MIMO-X}}$) in Figure 2.1 was calculated for the case of two pairs of transmitters-receivers with the same number A of transmit and receive antennas in [6], which is shown to be

$$\eta_{\text{MIMO-X}} = \frac{AMN}{M + N - 1} \tag{2.19}$$

$$= \frac{4}{3}A, \tag{2.20}$$

per orthogonal time and frequency dimension, when each node is equipped with A antennas. Notice that in the example in Figure 2.1 with two users, each transmitter/receiver needs at least three antennas for the system to have a DoF equal to four, which is required for the transmission of $s_{11}, s_{21}, s_{12}, s_{22}$ to be possible.

MIMO Interference Channel

The MIMO-IC can be considered as a particular case of the MIMO-X channel where the crossed links carry only interference and no useful information, i.e., each transmitter communicates information only to its desired receiver and subsequently generates interference to all the receivers.

A common scenario in the literature is the "K-User $M \times N$ MIMO Interference Channel", where there are K transmitters and K receivers, all of them with the same number of antennas M and N, respectively, and each transmitter j communicates with its corresponding receiver i while interfering with all other receivers. The literature so far has focused

mainly on the K-user $M \times N$ MIMO interference channel.

Cadambe and Jafar in [14] studied the DoF characterization of the wireless X network and they provided that the DoF outerbound of K-user X network as

$$\frac{K^2}{2K-1} \approx \frac{K}{2},\tag{2.21}$$

for large K. Since the K-user interference channel itself has $K/2$ DoFs, the outerbound implies that the X network loses its DoFs advantage over the interference network as K becomes large. The next section explains this model in more details.

2.2 System Model

The model for the wireless channel used throughout this work is the Rayleigh fading channel model [37]. The assumption at the basis of the Rayleigh fading model is that in a rich scattering environment the number of the reflected and scattered paths that contribute to each of the taps of the channel is large. For simplicity we also assume that the channel is flat-fading so that the channel is characterized by a single tap and the convolution operation reduces to a simple multiplication.

We consider the fading between each transmitter/receiver pair to be independent and the inputs of channel matrix $\mathbf{H}$ are circularly symmetric Gaussian random variables. The MIMO channel matrix $\mathbf{H}$ is generated randomly, but remains constant during each iteration. We can formulate mathematically for MIMO transmission structures the relation

$$\mathbf{Y} = \sqrt{\frac{\rho}{M}}\mathbf{H}\mathbf{X} + \mathbf{N},\tag{2.22}$$

where $\mathbf{Y}$ is received signal matrix, ρ is the SNR, $\mathbf{X}$ is the signal matrix with $M \times d$, $\mathbf{N}$ is the noise matrix with $\mathbb{E}\{\mathbf{N}\mathbf{N}^H\} = \sigma^2\mathbf{I}$ and $\mathbf{H} \in C^{N \times M}$ is given by

$$\mathbf{H} = \begin{bmatrix} h_{1,1} & h_{1,2} & \cdots & h_{1,M} \\ h_{2,1} & h_{2,2} & \cdots & h_{2,M} \\ \vdots & \vdots & \ddots & \vdots \\ h_{N,1} & h_{N,2} & \cdots & h_{N,M} \end{bmatrix},\tag{2.23}$$

with the power constraint

$$\frac{1}{M} \sum_{m=1}^{M} \mathbb{E}[|\mathbf{X}|_m^2] \leq P, \tag{2.24}$$

where P is the total power normalized for 1 and uniformly distributed for the M transmit antennas.

In the MIMO scenarios considered in this work we assume both that the antennas are sufficiently spaced from each other to ensure decorrelation of the channel elements as the case of correlated antennas. This is generally true since in a rich scattering environment the antenna spacing required for decorrelation is typically $\lambda/2$ where λ is the wavelength of the transmitted signal [38].

2.2.1 Correlation and CSIT

In order to model channel correlation (among the transmit antennas) we consider the Kronecker channel model [39]. Specifically the MIMO channel from transmitter j to receiver i is modeled as

$$\mathbf{H}_{ij} = \mathbf{H}_{ij}^{w} \mathbf{R}_t^{1/2} \qquad \forall i, j \in \{1, \dots, K\}, \tag{2.25}$$

where $\mathbf{H}_{ij}^{w} \sim \mathcal{CN}(\mathbf{0}, \mathbf{I})$ and $\mathbf{R}_t$ is a constant Hermitian Positive Semidefinite (PSD) matrix [40] representing the transmit antenna correlation (same matrix for all transmitters). The elements of $\mathbf{R}_t$ are calculated from a single correlation parameter ϕ, with the element (i, j) of $\mathbf{R}_t$ given by [41],

$$\mathbf{R}_t(i, j) = |\phi|^{|i-j|} \quad \text{for } i, j \in \{1, \dots, M\}, \tag{2.26}$$

where M is the number of transmit antennas. This model is widely used in the literature and industry and represents the correlation between elements of a uniform linear array of antennas where $\phi = 0$ and $|\phi| = 1$ correspond to no correlation and rank 1 channel, respectively [40].

Precise CSI at the transmitter is an unrealistic assumption in practical wireless systems. We model imperfect CSI through a Gauss-Markov uncertainty of the form [40]

$$\mathbf{H}_{ij}^{w} = \sqrt{1 - \beta^2} \tilde{\mathbf{H}}_{ij}^{w} + \beta \mathbf{E}_{ij}, \tag{2.27}$$

where $\mathbf{H}_{ij}^{w} \sim \mathcal{CN}(\mathbf{0}, \mathbf{I})$ is the true Gaussian part of the channel matrix,

$\tilde{\mathbf{H}}_{ij}^{w} \sim \mathcal{CN}(\mathbf{0}, \mathbf{I})$ is the imperfect observation of $\mathbf{H}_{ij}^{w}$ available to the nodes, and $\mathbf{E} \sim \mathcal{CN}(\mathbf{0}, \mathbf{I})$ is an i.i.d Gaussian noise term. The β parameter characterizes the partial CSI. That is, $\beta = 0$ corresponds to perfect channel knowledge, $\beta = 1$ corresponds to no CSI knowledge at the transmitter and values of $0 < \beta < 1$ account for partial CSI.

Taking channel correlation and CSI error into account, the full channel model is then given by

$$\mathbf{H} = \left(\sqrt{1 - \beta^2} \tilde{\mathbf{H}}^{w} + \beta \mathbf{E} \right) \cdot \mathbf{R}_t^{1/2}, \tag{2.28}$$

where the ij index was omitted for simplicity of notation.

2.2.2 K-user $M \times N$ MIMO Interference Channel

We consider a time-invariant interference wireless network consisting of K transmitter-receiver pairs, as shown in Figure 2.2. Each pair has M transmit and N receive antennas respectively, where each transmitter sends useful information only to its own receiver, while causing interference at the other receivers. This is the so called "K-user $M \times N$ MIMO Interference Channel" [3, 12, 13] and we refer to each transmitter-receiver pair as a *user*.

In order to account for the transmission of multiple streams per link we change the model from precoders/steering vectors (**v**/**u**) to precoders/steering matrices (**V**/**U**) and the transmit signal from scalar to a vector of transmit signals, denoted $\mathbf{s}_i$. The received signal vector at receiver i in Figure 2.2 is given by

$$\mathbf{y}_i = \underbrace{\mathbf{U}_i^H \mathbf{H}_{ii} \mathbf{V}_i \mathbf{s}_i}_{\text{desired signal}} + \underbrace{\sum_{\substack{k=1 \\ k \neq i}}^{K} \mathbf{U}_i^H \mathbf{H}_{ik} \mathbf{V}_k \mathbf{s}_k}_{\text{interference}} + \underbrace{\mathbf{U}_i^H \mathbf{n}_i}_{\text{noise}}, \tag{2.29}$$

where $\mathbf{U}_i^H$ is the linear receiver filter of *user* k with dimension $d_i \times N^{[i]}$, $\mathbf{H}_{ij}$ has dimension $N^{[i]} \times M^{[j]}$ ($N^{[i]}$ is the number of receive antennas of receiver i while $M^{[j]}$ is the number of transmit antennas of transmitter j), $\mathbf{s}_i$ has dimension $d_i \times 1$ (d_i is the number of degrees of freedom allocated for user i), $\mathbf{V}_i$ has dimension $M^{[i]} \times d_i$, and $\mathbf{y}_i, \mathbf{n}_i$ have, both, dimension equal to $N^{[i]} \times 1$.
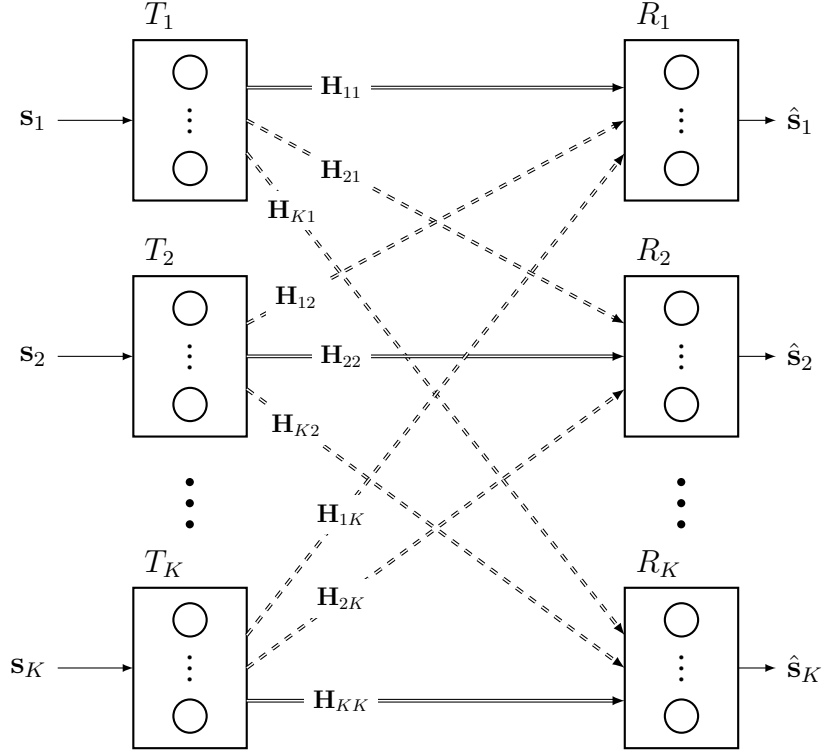
Figure 2.2 – MIMO Interference Channel with K users.

From (2.29), assuming the transmit symbol has unit variance for all users, we can see that the SINR at the i-th receiver is given by

$$\gamma_i = \frac{|\mathbf{U}_i^H \mathbf{H}_{ii} \mathbf{V}_i|^2}{\sum_{k \neq i} |\mathbf{U}_i^H \mathbf{H}_{ik} \mathbf{V}_k|^2 + ||\mathbf{U}_i||_2^2 \sigma^2} = \frac{S_i}{I_i + N_i}. \tag{2.30}$$

A possible overall system optimization objective is a function of the SINR at each receiver and corresponds to maximizing the sum-utility across users. That is, the optimization function is given by

$$\max_{\substack{\mathbf{V}_1 \ldots \mathbf{V}_j \\ \mathbf{U}_1 \ldots \mathbf{U}_j}} \sum_{i=1}^{K} f_i(\gamma_i) \quad \text{s.t.:} \quad ||\mathbf{V}_j||_2^2 \leq P_j^{\max} \quad \forall j \in \{1, \ldots, K\}, \tag{2.31}$$

where $P_j^{\max}$ denotes the power constraint of transmitter j.

The properties of this optimization problem depend on the utility functions employed, since due to interference it may have multiple locally optimal solutions [42]. However, for a wide class of utility functions the constraint set is convex yielding a unique local optimum, which is

also the global optimum and can be solved using standard optimization techniques.

2.2.3 Degrees of Freedom for the K-user $M \times N$ MIMO Interference Channel

Initially, the DoF for the MIMO-IC ($K = 2$) was found in [43] for the general case of different number of transmit and receive antennas ($M^{[i]}, N^{[i]}$) and is given by

$$\eta_{\text{MIMO-IC}_2} = \min[M_1 + M_2, \ N_1 + N_2, \ \max(M_1, N_2), \ \max(M_2, N_1)]. \qquad (2.32)$$

Generalizing, the DoF characterization of the Single-Input Single-Output (SISO) ($M = N$) to the K-user MIMO Interference Channel when all nodes have the same number of antennas was show in [12] to be equal to

$$\eta_{\text{MIMO-IC}_K} = \frac{KM}{2}, \qquad (2.33)$$

which is equal to (2.32) when $K = 2$ and all transmitters/receivers have the same number of antennas M. Note that in both of the previous mentioned cases the DoF for the MIMO-IC is lower than the DoF for the MIMO-X channel, which is expected since the former is a particular case of the latter.

The characterization of the DoF of MIMO interference channels is more challenging when all the nodes do not have the same number of antennas. Gou and Jafar have shown in [13] that the K-user $M \times N$ MIMO interference channels are found when the ratio

$$R = \frac{\max(M, N)}{\min(M, N)} \qquad (2.34)$$

is an integer. There is no DoF penalty from interference while the number of users $K \leq R$, i.e., zero forcing suffices and everyone gets $\min(M, N)$ DoF. On the other hand, when $K \geqslant R + 1$, the DoF per user is again not limited by the number of users, and everyone gets $\min(M, N)\dfrac{R}{R + 1}$ DoF with an appropriate technique called interference alignment.

2.3 Interference Alignment

The principle of interference alignment consists in the basic idea of constructing transmit signals in such a way that the interference they

cause at all unintended receivers overlaps onto the same subspace, while they still remain separable at the intended receivers [43].
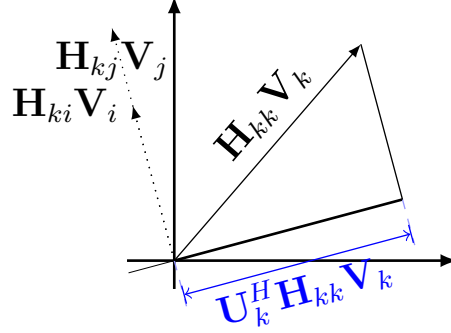
Figure 2.3 – Perfect alignment at receiver k of the interference caused by transmitters i and j.

Figure 2.3 depicts the perfect alignment of the interference caused by transmitters i and j at the receiver k. Note that the precoders $\mathbf{V}_j$ and $\mathbf{V}_i$ align the cross-channels $\mathbf{H}_{kj}$ and $\mathbf{H}_{ki}$, respectively, in the same subspace, represented by the dotted line. On the other hand, the precoder $\mathbf{V}_k$ does not project the direct channel $\mathbf{H}_{kk}$ in any particular direction since $\mathbf{V}_k$ is intended to only align the interference at receivers j and i. Due to the randomness of the channel, the equivalent channel $\mathbf{H}_{kk}\mathbf{V}_k$ is likely to span the whole space.

At the receiver k the ZF filter $\mathbf{U}_k$ will simply project the received signal (2.29) in the space orthogonal to the interference space, thus eliminating all the interference. Mathematically, the interference alignment conditions are given by [8]

$$\mathbf{U}_i^H \mathbf{H}_{ij} \mathbf{V}_j = 0, \ \forall j \neq i \tag{2.35}$$

$$\text{rank}\left(\mathbf{U}_i^H \mathbf{H}_{ii} \mathbf{V}_i\right) = d. \tag{2.36}$$

That is, the desired signals are received through a $d \times d$ full rank channel matrix [8]

$$\overline{\mathbf{H}}_{ii} \triangleq \mathbf{U}_i^H \mathbf{H}_{ii} \mathbf{V}_i, \tag{2.37}$$

while the interference is completely eliminated.

Note that when all elements of the channel matrices are random and independently generated from a continuous distribution and $\mathbf{U}_j$ and $\mathbf{V}_j$ can be found to satisfy (2.35), then (2.36) will be automatically satisfied with probability one [8]. However, this is not true if the channel has

some particular structure, as in the case of interference alignment in the frequency domain, where the channel is a diagonal matrix.

Furthermore, the feasibility conditions of equations (2.35) and (2.36) are the same for the direct and reverse channels. Hence, if a set of degrees of freedom is feasible on the original interference network then it is also feasible for the reciprocal interference network. This reciprocity of the interference alignment is a key property used in [8] and many other papers in the literature to address the distributed scenario.

2.3.1 Feasibility Conditions

In order to determining the feasibility, we must account for the number of equations and variables. Thus, to determine the feasibility condition for diversity interference alignment, our task becomes calculating and comparing the number of equations and the number of variables of the multivariate polynomial system corresponding to a interference alignment scheme [44].

Considering (2.35) for all interference links and (2.36) for the desired links, a linear system of equations can be formulated. We can rewrite the conditions in (2.35) as follows [45]

$$(\mathbf{u}_i^m)^H \mathbf{H}_{kj} \mathbf{v}_j^n = 0, \ \forall j \neq k \in \mathcal{K} = \{1, 2, \ldots, K\} \tag{2.38}$$
$$\forall n \in \{1, 2, \ldots, d_j\} \quad \text{and} \quad \forall m \in \{1, 2, \ldots, d_k\}$$

where $\mathbf{v}_j^n$ and $\mathbf{u}_i^m$ are the transmit and receive beamforming vectors (columns of precoding and interference suppression filters, respectively). Hence, N_e equations are directly obtained from (2.38) which can be expressed as follows [7]

$$N_e = \sum_{\substack{k,j \in \mathcal{K} \\ k \neq j}} d_k d_j. \tag{2.39}$$

However, the number of variables can not be obtained easily because we have to be careful not to count any superfluous variables that do not help with interference alignment.

Then, we count the number of variables of this multivariate polynomial system. For a given set of channel matrices, d_k can be completely described by $\mathbf{H}_{ij}$ and $\mathbf{v}_i$, for $1 \leq i, j \leq K$, and can not be counted as an independent variable. Thus, all the variables of this multivariate polynomial system come from the precoding and receiving filters.

The signal space of the precoding filters for each transmitter with M antennas, after removing the effect of the superfluous variables, can provide $d_k(M - d_k)$ variables. Similarly, each receiving filter with N antennas can provide $d_k(N - d_k)$ variables. Thus, the total number of variables N_v introduced by all precoding and receiving filters in the network to be designed is [7]

$$N_v = \sum_{k=1}^{K} d_k(M + N - 2d_k). \tag{2.40}$$

For symmetric systems, simply comparing the total number of equations and the total number of variables is sufficient to determine whether the system is proper or improper. In order to obtain an IA solution, we need

$$N_v \geqslant N_e$$

$$\sum_{k=1}^{K} d_k(M + N - 2d_k) \geqslant \sum_{\substack{k,j \in \mathcal{K} \\ k \neq j}} d_k d_j$$

$$M + N - (K + 1)d \geqslant 0. \tag{2.41}$$

Otherwise, the system is not feasible.

In the next chapter, we present the closed-form solution for the case largely explored in the literature.

2.4 Remarks and Conclusions

In this chapter we introduced a technical background with some fundamental concepts to understand the IA. Initially we presented the definition of DoF and the possible scenarios of IA. Then, the description of the system model was shown in order to emphasize the necessary conditions for IA. Finally, we reported an approach for the channel correlation and CSI considering its impact on the performance of IA.

Chapter 3

Closed-Form Solutions and Algorithms for MIMO Interference Alignment Systems

Interference alignment schemes are presented in [12] in the form of closed-form expressions for the transmit precoding matrices. However, they require global channel knowledge which can be an overwhelming overhead in practice. In general, analytical solutions to the interference alignment problem are difficult to obtain and even the feasibility of IA over a limited number of signaling dimensions is an open problem [8].

Therefore, previous studies have proposed some alternative algorithms with the objectives of requiring only local channel knowledge at each node and providing numerical insights into the feasibility of alignment.

3.1 Closed-Form Solutions for Interference Alignment

There are few closed-form, i.e., analytical solutions to the IA problem while several iterative solutions have been explored in the literature. It is an intuitive brute force approach, to write the alignment conditions and attempt to solve the desired variables. Deriving a closed-form interference alignment solution, assuming constant-coefficient channels, is difficult for more than 3 users due to the interdependence of each precoder and receiver interference-free subspace [9]. Therefore, we illustrate hereafter this method for the case of $K = 3$.

3.1.1 Closed-form beamforming design for three-user MIMO System

The interference alignment can be used in SISO IC through symbol extension of the channel, which can be made in time-slots or

frequency-slots. On the other hand, it is not necessary at multiple antenna nodes ($M > 1$). Considering an $(M \times N, d)^K$ MIMO IC system, we can limit this analysis for a symmetric system, i.e., all the nodes are equipped with $M = N$ antennas (transmitters and receivers). As a consequence, the DoF assignment $(d_{[1]}, \dots, d_{[K]})$ is symmetric, i.e., $d_{[1]} = \cdots = d_{[K]} = d$.

According to (2.41), for a symmetric system the last inequality translates into $2M \geqslant (K+1)d$. The feasibility of IA when we can achieve the total DoF replacing d by $M/2$ in the previous inequality yields an upper bound on K, which is 3. Thus, the $(M \times M, M/2)^K$ system admits solution and it is feasible to design beamforming vectors for IA, that achieve the full DoF when $K \leq 3$. For any K, the total DoF can be obtained and it was proved to be $KM/2$ by Cadambe and Jafar in [12]. We present the proof for 3-user MIMO IC with M antennas in each node when M is even because the case when M is odd is more complicated due to the use of a 2-symbol extension.

Following (2.29), we knew that to enable the receiver to decode $M/2$ data streams from the $M \times 1$ received signal vector $\mathbf{y}_i$, the interference signal space should have at most $M/2$ dimensions and be linearly independent with the desired signal space. Thus, each precoder has to be designed to satisfy the three interference aligning constraints described as [46]

$$\text{span}(\mathbf{H}_{12}\mathbf{V}_2) = \text{span}(\mathbf{H}_{13}\mathbf{V}_3),$$
$$\text{span}(\mathbf{H}_{21}\mathbf{V}_1) = \text{span}(\mathbf{H}_{23}\mathbf{V}_3),$$
$$\text{span}(\mathbf{H}_{31}\mathbf{V}_1) = \text{span}(\mathbf{H}_{32}\mathbf{V}_2), \tag{3.1}$$

where $\text{span}(X)$ indicates the vector space spanned by the column vectors of X.

This system of equations is computationally infeasible to determine the precoders because there are infinite sets of solutions to satisfy this problem. Then, to compute the proper precoding matrices, the IA method

restricts the above constraints as

$$\text{span}(\mathbf{H}_{12}\mathbf{V}_2) = \text{span}(\mathbf{H}_{13}\mathbf{V}_3),$$
$$\mathbf{H}_{21}\mathbf{V}_1 = \mathbf{H}_{23}\mathbf{V}_3,$$
$$\mathbf{H}_{31}\mathbf{V}_1 = \mathbf{H}_{32}\mathbf{V}_2. \tag{3.2}$$

Through these restrictions we can limit the infinite sets of solutions, since we allow to select randomly values of $\mathbf{V}_2$ or $\mathbf{V}_3$ to determine the remaining precoders.

In addition, the reception matrices are designed such that they can be equivalently expressed as

$$\text{span}(\mathbf{V}_1) = \text{span}(\mathbf{E}\mathbf{V}_1), \tag{3.3}$$
$$\mathbf{V}_2 = \mathbf{F}\mathbf{V}_1, \tag{3.4}$$
$$\mathbf{V}_3 = \mathbf{G}\mathbf{V}_1, \tag{3.5}$$

where

$$\mathbf{E} = (\mathbf{H}_{31})^{-1}\mathbf{H}_{32}(\mathbf{H}_{12})^{-1}\mathbf{H}_{13}(\mathbf{H}_{23})^{-1}\mathbf{H}_{21},$$
$$\mathbf{F} = (\mathbf{H}_{32})^{-1}\mathbf{H}_{31};$$
$$\mathbf{G} = (\mathbf{H}_{23})^{-1}\mathbf{H}_{21}.$$

Finally, $\mathbf{V_1}$ is chosen as

$$\mathbf{V}_1 = [\mathbf{e}_1\ \mathbf{e}_2 \cdots \mathbf{e}_{M/2}], \tag{3.6}$$

where $\mathbf{e}_1\ \mathbf{e}_2 \cdots \mathbf{e}_{M/2}$ are the eigenvectors of $\mathbf{E}$. $\mathbf{V}_2$ and $\mathbf{V}_3$ can be obtained by (3.4) and (3.5).

3.2 Algorithms for MIMO Interference Channels

Although interference alignment can be applied in different scenarios, each one with its own model, a common structure is shared among the different algorithms with the used metric being the main variation. Each algorithm is designed to optimize a global objective $\mathcal{J}$ that incorporates the performance of each data link in the network whose goal of is to minimize the total "leakage interference" that remains at each receiver after attempting to cancel the coordinated interference [9].

Early in the classical approaches of interference alignment, the idea was to perfectly align the full interference inside one dimension. However, the literature evaluated that relaxing these constraints has allowed to obtain improvement of the results.

The mathematical representation of interference alignment is realized through a global optimization function given by

$$
\mathcal{J}_{\text{IA}} = \sum_{k=1}^{K} \mathbb{E} \left\{ \left\| \mathbf{U}_k^H \sum_{\substack{\ell=1 \\ \ell \neq k}}^{K} \mathbf{H}_{k,\ell} \mathbf{V}_\ell d_\ell \right\|_F^2 \right\}, \tag{3.7}
$$

where $|| \cdot ||_F$ denotes the Frobenius norm. Each algorithm is designed to optimize a global objective $\mathcal{J}_{\text{IA}}$ that incorporates the performance of each data link in the network.

Evaluating the expectation and exploiting independence of the signals, the optimization problem can be expressed, respecting the per-stream power constraint, as

$$
\begin{aligned}
\min_{\{\mathbf{V}_l\},\{\mathbf{U}_k\}} \quad & \mathcal{J}_{\text{IA}} = \sum_{k=1}^{K} \sum_{\substack{\ell=1 \\ \ell \neq k}}^{K} ||\mathbf{U}_k^H \mathbf{H}_{k,\ell} \mathbf{V}_\ell||_F^2 \\
\text{subject to} \quad & \mathbf{V}_\ell^H \mathbf{V}_\ell = \frac{\rho_\ell}{S_\ell} \mathbf{I}, \ell \in \{1, \dots, K\} \\
& \mathbf{U}_k^H \mathbf{U}_k = \mathbf{I}, k \in \{1, \dots, K\}.
\end{aligned} \tag{3.8}
$$

In general, analytical solutions (closed-form solutions) are difficult to obtain and even the feasibility of interference alignment over a limited number of signaling dimensions is an open problem. The different algorithms in the literature can be roughly divided into two classes: centralized and distributed algorithms.

Several papers in the literature work with the centralized case where each transmitter has global channel knowledge in order to perform the interference alignment when it is feasible. On the other hand, for the distributed case each transmitter must know only its direct channel matrix and combined cross-channel-receiver gains to neighboring receivers. The distributed case has a more practical appeal and has received more and more attention lately. Due to the complexity, closed-form solutions for the MIMO-IC are known only for the cases up to three interfering nodes. Therefore, we focus on these cases. The

centralized algorithms are described in Section 3.2.1 while the distributed algorithms are described in Section 3.2.2.

3.2.1 Centralized Algorithms

Centralized algorithms require global channel knowledge at each node, which can be considered an overwhelming overhead in practice [8]. However, the first studies on interference alignment focused on them and there are even some closed-form expressions for the transmit precoding matrices [12, 43]. The idea is to find a precoding matrix at each user that aligns the interference at all receivers to within $M - d$ dimensions, while keeping the d-dimensional desired signal space linearly independent of the interference subspace, for an appropriately chosen d [47].

According to the previous section, to provide closed-form expressions for the precoding matrices is complex. Thus, there is interest in finding precoders for the interference channels through computational algorithms that benefit from the non-optimality of interference alignment for low to medium SNR values. In the following, centralized interference alignment algorithms are described, while distributed algorithms are described in Section 3.2.2.

IA-ZF Precoding

Linear precoding at the transmitters and zero-forcing filtering at the receivers is one way to achieve the total DoF promised by IA. An important problem is to devise algorithms for computing the transmit precoding matrices and the receive filtering matrices that align the interferences at all the receivers, given the channel state information [47].

In general, the reception matrices are designed such that:

$$\begin{aligned}
\mathbf{U}_1[\mathbf{H}_{12}\mathbf{V}_2 \quad \mathbf{H}_{13}\mathbf{V}_3] &= \mathbf{0}, \\
\mathbf{U}_2[\mathbf{H}_{21}\mathbf{V}_1 \quad \mathbf{H}_{23}\mathbf{V}_3] &= \mathbf{0}, \\
\mathbf{U}_3[\mathbf{H}_{31}\mathbf{V}_1 \quad \mathbf{H}_{32}\mathbf{V}_2] &= \mathbf{0}.
\end{aligned} \tag{3.9}$$

Since the interference is completely eliminated by the ZF-IA algorithm, considering the constraints in Equation (3.2), the previous relation can be written as:

$$\begin{aligned}
\mathbf{U}_1[\mathbf{H}_{12}\mathbf{V}_2] &= \mathbf{0}, \\
\mathbf{U}_2[\mathbf{H}_{21}\mathbf{V}_1] &= \mathbf{0}, \\
\mathbf{U}_3[\mathbf{H}_{31}\mathbf{V}_1] &= \mathbf{0}.
\end{aligned} \tag{3.10}$$

By calculating the precoder and receiver matrices for different subsets of eigenvectors of $\mathbf{E}$ according to Section 3.1.1, we can choose the solution that maximizes the minimum SINRs of all streams in order to achieve better performance. The IA-ZF strategy is summarized in Algorithm 3.1.

An example can be considered for the system model in which there are two base stations and two mobile users. Each base station and each mobile user has three antennas. While each base station transmits two data streams to different mobile users, each mobile user receives two data streams from the two different base stations.

Algorithm 3.1 Interference Alignment with Zero-Forcing criterion.

  i. Assign one eigenvector of matrix $\mathbf{E}$ for the matrix $\mathbf{V}_1$;

  ii. Use (3.4) and (3.5) to obtain $\mathbf{V}_2$ and $\mathbf{V}_3$, respectively;

  iii. Calculate the reception matrix $\mathbf{U}_i$ according to (3.10);

  iv. Calculate the minimum SINRs of the users. If it is greater than previous value store the matrices $\mathbf{U}_1, \mathbf{U}_2, \mathbf{U}_3, \mathbf{V}_1, \mathbf{V}_2, \mathbf{V}_3$;

  v. Repeat from step **ii** until all eigenvectors of $\mathbf{E}$ are tested.

In order to fully eliminate the interference between the four streams, the precoding vectors and the receive steering vectors must satisfy Equations (2.15)-(2.18). In the system performance optimization, the algorithm also maximizes the minimum of the SINRs of the four streams.

IA-MMSE Precoding

This design criterion aims at minimizing the mean square error (MSE) of the detected data. For the kth user, the mean square error MSE_k can be calculated as [48]

$$MSE_k = \mathbb{E}\{|\hat{\mathbf{y}}_k - \mathbf{y}_k|^2\} = \mathbb{E}\{\mathrm{Tr}[(\hat{\mathbf{y}}_k - \mathbf{y}_k)(\hat{\mathbf{y}}_k - \mathbf{y}_k)^H]\}, \tag{3.11}$$

where the $\mathrm{Tr}(\cdot)$ operator represents the trace.

Then, the optimization problem is given by [48]

$$\min_{\{\mathbf{V}_k\},\{\mathbf{U}_k\}} \sum_{k=1}^{K} \mathrm{MSE}_k \tag{3.12}$$
$$\text{subject to} \quad \mathrm{Tr}(\mathbf{V}_k^H \mathbf{V}_k) = P_k, \quad \forall k \in \{1,\ldots,K\}.$$

The Lagrange dual objective function can be constructed as [36, 48]

$$L(\mathbf{V}_k; \mathbf{U}_k; \lambda_k) = \sum_{k=1}^{K} MSE_k + \sum_{k=1}^{K} \lambda_k [\text{Tr}(\mathbf{V}_k^H \mathbf{V}_k) - P_k], \qquad (3.13)$$

where λ_k is the Lagrange multiplier associated with the power constraint of transmitter k.

According to Karush-Kuhn-Tucker (KKT) conditions [48]:

$$\frac{\partial L}{\partial \mathbf{V}_k} = \mathbf{0}, \quad \forall k \in \{1, \ldots, K\}, \qquad (3.14)$$

$$\frac{\partial L}{\partial \mathbf{U}_k} = \mathbf{0}, \quad \forall k \in \{1, \ldots, K\}, \qquad (3.15)$$

$$\frac{\partial L}{\partial \lambda_k} = \mathbf{0}, \quad \forall k \in \{1, \ldots, K\}. \qquad (3.16)$$

We can get the following equations in [48]:

$$\mathbf{V}_k = \left(\sum_{i=1}^{K} \mathbf{H}_{ik}^H \mathbf{U}_i^H \mathbf{U}_i \mathbf{H}_{ik} + \lambda_k \mathbf{I} \right)^{-1} \mathbf{H}_{kk}^H \mathbf{U}_k^H, \quad \forall k \in \{1, 2, \ldots, K\} \qquad (3.17)$$

and

$$\mathbf{U}_k = \mathbf{V}_k^H \mathbf{H}_{kk}^H \left(\sum_{i=1}^{K} \mathbf{H}_{ki}^H \mathbf{V}_i \mathbf{V}_i^H \mathbf{H}_{ki}^H + \sigma_n^2 \mathbf{I} \right)^{-1}, \quad \forall k \in \{1, 2, \ldots, K\} \qquad (3.18)$$

and

$$\text{Tr}(\mathbf{V}_k^H \mathbf{V}_k) = P_k, \quad \forall k \in \{1, \ldots, K\}. \qquad (3.19)$$

The case considering the MIMO-X channel composed by two pairs transmitter/receiver with three antennas for each one sending a total of four streams is given by [36]

$$\begin{aligned} \min_{\{\mathbf{V}_k\},\{\mathbf{U}_k\}} \quad & \sum_{k=1}^{4} \text{MSE}_k \\ \text{subject to} \quad & \text{Tr}\left(\sum_{i=1}^{2} \mathbf{v}_i^H \mathbf{v}_i \right) = \text{Tr}\left(\sum_{i=3}^{4} \mathbf{v}_i^H \mathbf{v}_i \right) = P, \end{aligned} \qquad (3.20)$$

where $\mathbf{v}_3 = \mathbf{T}_1 \mathbf{v}_1$, $\mathbf{v}_4 = \mathbf{T}_2 \mathbf{v}_2$, P is the same transmit power for each base station, $\mathbf{T}_1 = (\mathbf{H}_{22})^{-1} \mathbf{H}_{12}$ and $\mathbf{T}_2 = (\mathbf{H}_{21})^{-1} \mathbf{H}_{11}$.

The IA-MMSE Precoding [48] scheme is described in Algorithm 3.2. It was proposed in order to overcome the difficulty to determine the optimal transmit precoding matrix $\mathbf{V}_k$ for each user depending mutually on the optimal receiving filter matrices $\mathbf{U}_k$ for all users.

Algorithm 3.2 Interference Alignment with MMSE criterion.

  i. Initialize the precoder matrices $\mathbf{V}_k$;

  ii. Calculate the receiver vectors, $\mathbf{U}_k$,using (3.18);

  iii. Solve λ_k by replacing (3.17) on the power constraint of user k.

  iv. Update $\mathbf{V}_k$ according to (3.17) with solved λ_k;

  v. Repeat from step **ii** until convergence.

We present as illustration a simulation result of centralized algorithms in the MIMO-X scenario. This scenario was illustrated in Figure 2.1, where all transmitters and receivers have three antennas and 100 symbols (4-PSK modulation) were transmitted for each simulation snapshot. The Bit Error Rate (BER) curves as a function of $\frac{E_b}{N_0}$ are depicted in Figure 3.1 for the IA-ZF and MMSE precoding algorithms.
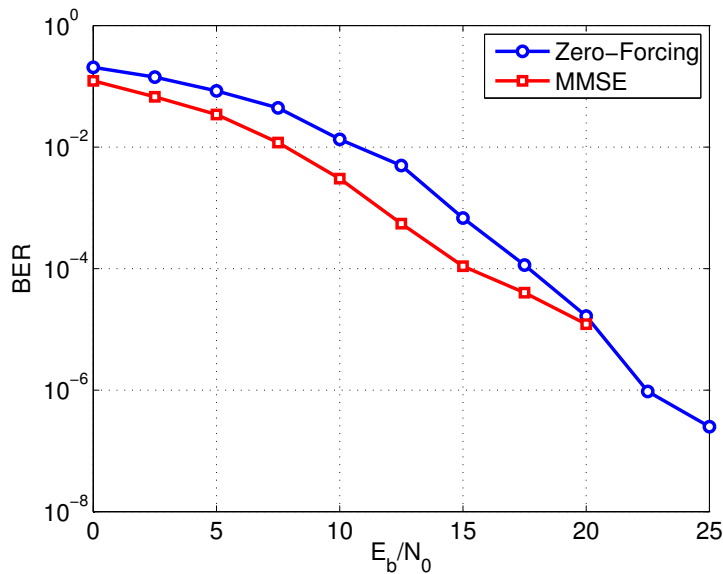

Figure 3.1 – Results obtained using the algorithm IA-ZF and IA-MMSE precoding with 50 iterations.

Comparing the obtained results with the ones in [36] we found that the BER curves matched, thus confirming the validation of the results. The simulation results obtained with the algorithm IA-ZF and IA-MMSE are shown to consolidate our preliminary interpretation about the behavior of the mentioned algorithms. In the next section, we are going to focus our attention on distributed algorithms, as well as using more realistic channel models.

3.2.2 Distributed Algorithms

Distributed algorithms that require only local channel knowledge at each transmitter have a more practical appeal than the centralized algorithms. A centralized scheme for resource allocation requires excessive information exchange and overhead for most practical networks. In addition, depending on the objective and specific resource constraints, the centralized optimization problem can be non-convex with associated worst-case complexity that increases exponentially with the number of users and DoFs [42].

Furthermore, due to the complexity in providing closed-form expressions for the precoding matrices and the non-optimality of interference alignment for low to medium SNR values, there is interest in finding precoders for the interference channel that relax the perfect alignment constraint with the goal of obtaining better and non-asymptotic sum rate performance. Hereafter, we provide precoder solutions in a practical setting and take advantage of their flexibility in application to arbitrary networks for which closed-form solutions are unknown.

3.2.3 Pricing Algorithm

In the *distributed interference pricing* algorithm [19, 42, 49–51], the optimization problem in (2.31) is broken down into optimizing the precoders $\mathbf{v}_k$ and optimizing the receive filters $\mathbf{u}_k$. Therefore, the optimization of the precoders is formulated in a distributed approach as

$$\max_{\mathbf{v}_k} f_k\left(\gamma_k\right) - \sum_{j \neq k} \pi_j |\mathbf{u}_j^H \mathbf{H}_{jk} \mathbf{v}_k|^2 \quad \text{s.t.} \quad ||\mathbf{v}_k||_2^2 \leq P_k^{\max}, \tag{3.21}$$

where the utility function $f_k(\cdot)$ is a function of the SINR γ_k and measures the quality of service of the user k. The second term in (3.21) corresponds to the cost for the transmitter k to cause interference at the unintended

receivers and it depends on the values π_j ($j \neq k$) announced by them. In other words, the user's payoff is its utility minus the total cost summed over all unintended receivers.

Due to the required excessive information exchange for the transmitter to predict the exact effect caused by the interference, each receiver announces a single interference price. The interference price for a user j is calculated by

$$\pi_j = -\frac{\partial f_j\left(\gamma_j\right)}{\partial I_j}, \tag{3.22}$$

which is the marginal cost of his own utility per unit interference. The utility function f_k is assumed to be a monotonically increasing, concave and twice differentiable function of γ_k.

Traditionally the rate utility, $f_k = \log(1 + \gamma_k)$, is utilized because it corresponds to the Shannon capacity of the channel, since the interference is treated as additive Gaussian noise. This is also employed in the original interference pricing algorithm. Thus, the interference price π_k results in

$$\pi_{k_{\text{rate}}} = \frac{I_k + N_k}{I_k + N_k + S_k} \cdot \frac{-S_k}{(I_k + N_k)^2}. \tag{3.23}$$

There are several utility functions which can be used to replace the rate utility and it is interesting to note that the prices π_j yield a balance between maximizing the utility function $f_k(\gamma_k)$ (egoistic objective) and minimizing the interference caused at the unintended receivers (altruistic objective). In general, any sensible utility function should be non-decreasing in the SINR. However, some criteria must be satisfied by the utility functions to prove convergence of the distributed pricing algorithms. The proof for these algorithms can be seen in [42].

Furthermore, other aspects such as the fairness in the distributed resources can be analyzed and their corresponding interference prices in the pricing algorithm regarding the obtained system performance. An example is the "α-fair" utility function given by [52]

$$f(\gamma_k) = \frac{\gamma^\alpha}{\alpha}, \quad 0 < \alpha < 1, \tag{3.24}$$

for which the corresponding interference price can then be derived as

$$\pi_{k_{\alpha\text{-fair}}} = \left(\frac{S_k}{I_k + N_k}\right)^{\alpha - 1} \frac{S_k}{(I_k + N_k)^2}. \tag{3.25}$$

The "α-fair" utility "flattens out" at high SINRs when $\alpha \leq 1$ and therefore reflects an application that becomes insensitive to rate.

In [50], a numerical algorithm for solving the nonlinear optimization problem in (3.21) is presented, where the KKT conditions for user k are given by

$$\underbrace{\left[a_k(\mathbf{v}_k)\mathbf{H}_{kk}^H\mathbf{u}_k\mathbf{u}_k^H\mathbf{H}_{kk} - \sum_{i \neq k} \pi_i \mathbf{H}_{ik}^H\mathbf{u}_i\mathbf{u}_i^H\mathbf{H}_{ik} \right]}_{\mathbf{X}_k} \mathbf{v}_k = \lambda_k\mathbf{v}_k, \qquad (3.26)$$

with

$$a_k(\mathbf{v}_k) = \frac{f_k'(\gamma_k)}{|\mathbf{u}_k^H\mathbf{n}_k|^2 + \sum_{i \neq k} |\mathbf{u}_k^H\mathbf{H}_{ki}\mathbf{v}_i|}, \qquad (3.27)$$

where λ_k is the Lagrange multiplier associated with the power constraint, and f_k' is the first derivative of the utility function $f_k(\gamma_k)$ with respect to γ_k.

Considering the MMSE criterion, the optimal receive filter for user k is given by [50]

$$\mathbf{u}_{\text{MMSE},k} = \left(\sum_{j=1}^{K} \mathbf{H}_{kj}\mathbf{v}_j\mathbf{v}_j^H\mathbf{H}_{kj}^H + \sigma^2\mathbf{I} \right)^{-1} \mathbf{H}_{kk}\mathbf{v}_k. \qquad (3.28)$$

The iterative algorithm is summarized by Algorithm 3.3.

Algorithm 3.3 Distributed Interference Pricing.

---

  i. Initialize randomly a beamforming vector $\mathbf{v}_k$ for each user k respecting the power constraint;

 ii. Then, optimize the receive filter $\mathbf{u}_k$ according to (3.28);

iii. Each receiver k calculates the interference price π_k and announces it to other users;

 iv. A random user is chosen to solve (3.21) and optimize his beamforming vector according to (3.26);

  v. The remaining users update their receive filters using (3.28);

 vi. Repeat from step **ii** until convergence.

The form of an eigenvector equation is found in (3.26). If all eigenvalues of $\mathbf{X}_k$ are negative, then the updated precoder $\mathbf{v}_k$ is the zero vector, otherwise, it is the eigenvector associated with the largest eigenvalue of $\mathbf{X}_k$ with an appropriate scale factor. In Chapter 5, we show the obtained simulation results.

3.2.4 IA Alternating Algorithm

The IA alternating approach general idea is to align the interference at each receiver by adjusting their interference subspace via an alternating optimization. In [9, 40, 53] a general algorithm with varying performance and complexity trade-offs is proposed for the MIMO interference channel based on an alternating minimization over the precoding matrices at the transmitters and the interference subspaces at the receivers, which is proven to converge.

For the ith user (transmitter/receiver pair) the alternating minimization method results in a unitary precoder $\mathbf{V}_i$, and a set of non-unique orthogonal bases for the interference subspace, i.e., columns of $\mathbf{C}_i$, such that [40]

$$\mathbf{V}_i^H \mathbf{V}_i = \mathbf{C}_i^H \mathbf{C}_i = \mathbf{I} \quad \forall i \in \{1, \ldots, K\}. \tag{3.29}$$

Assuming the alternating minimization algorithm has converged to an IA solution, by knowing a basis for the interference subspace at each receiver i, i.e., the columns of $\mathbf{C}_i$, the received signal at the ith user in a MIMO IC system can be written as

$$\mathbf{y}_i = \mathbf{H}_{ii}\mathbf{V}_i\mathbf{x}_i + \mathbf{C}_i \sum_{k \neq i}^{K} \mathbf{A}_{ik}\mathbf{x}_k + \mathbf{n}_i = \tilde{\mathbf{H}}_i \begin{bmatrix} \mathbf{x}_i \\ \sum_{k \neq i}^{K} \mathbf{A}_{ik}\mathbf{x}_k \end{bmatrix} + \mathbf{n}_i, \tag{3.30}$$

where $\mathbf{A}_{ik}$ determines the interference from transmitter k at receiver i and is given by $\mathbf{C}_i\mathbf{A}_{ik} = \mathbf{H}_{ik}\mathbf{V}_k$ and $\tilde{\mathbf{H}}_i \triangleq [\mathbf{H}_{ii}\mathbf{V}_i, \ \mathbf{C}_i]$ is the effective channel at receiver i. For the IA solution, each user needs to determine its interference subspace, where undesirable users should project their signals while it needs to project its own signal into the interference subspace of the other users. These two steps are performed until the algorithm converges.

The measure that calculates the error between $\mathbf{A}$ and its closest point

on $\mathcal{W}$ is

$$d(\mathbf{A}, \mathcal{W}) = ||\mathbf{A} - \tilde{\mathbf{A}}||_F^2, \qquad (3.31)$$

where $\mathbf{A} \in \mathcal{C}^{N \times q}$, $\mathcal{W}$ is the p-dimensional linear subspace of an $N-$dimensional complex space $(p \geqslant q)$ and $\tilde{\mathbf{A}}$ is the orthogonal projection of $\mathbf{A}$ onto $\mathcal{W}$, which is given by

$$\tilde{\mathbf{A}} = \mathbf{W}\mathbf{W}^H \mathbf{A}, \qquad (3.32)$$

where $\mathbf{W}$ is an orthonormal basis of $\mathcal{W}$.

The IA algorithm proposed in [53] for the MIMO IC is then formulated as optimizing the measure between a matrix and a subspace. That is, solving the problem

$$\min_{\substack{\mathbf{V}_l^H \mathbf{V}_l = \mathbf{I}, \forall l \\ \mathbf{C}_k^H \mathbf{C}_k = \mathbf{I}, \forall k}} \sum_{k=1}^{K} \sum_{\substack{l=1 \\ l \neq k}}^{K} ||\mathbf{H}_{k,l}\mathbf{V}_1 - \mathbf{C}_k \mathbf{C}_k^H \mathbf{H}_{k,l}\mathbf{V}_l||_F^2. \qquad (3.33)$$

In order to solve (3.33), we can optimize the objective function for one variable, alternating between which variables are held fixed and which are optimized. Thus, the alternating minimization takes the following form:

Algorithm 3.4 Interference Alignment via Alternating Minimization.

  i. Fix $\mathbf{V}_l$ arbitrarily for all l;

  ii. Let the columns of $\mathbf{C}_k$ be the $N_k - S_k$ dominant eigenvectors of $\sum_{k \neq l} \mathbf{H}_{k,l}\mathbf{V}_l\mathbf{V}_l^H\mathbf{H}_{k,l}^H$;

  iii. Let the columns of $\mathbf{V}_l$ be the S_l dominant eigenvectors of $\sum_{l \neq k} \mathbf{H}_{k,l}^H(\mathbf{I}_{N_k} - \mathbf{C}_k\mathbf{C}_k^H)\mathbf{H}_{k,l} \quad \forall l$;

  iv. Repeat steps **ii** and **iii** until convergence.

An interesting feature of the Algorithm 3.4 is that it can be used for any number of users, method of obtaining CSI, reciprocity of the channel, antenna distribution or stream allocation, as long as the IA problem is feasible, which is not the case of Algorithms 3.1 and 3.2.

Considering the presence of the external interference, the performance achieved by the previous algorithm would have a very strong degradation.

A way to overcome this issue is to use the same framework of the alternating algorithm and take into account the external interference directions in the choice of the optimal interference subspace, as it is described in [9].

Thus, similarly to the conventional IA alternating approach and treating both internal and external interference the minimization problem can be rewritten as:

$$\min_{\substack{\mathbf{V}_l^H \mathbf{V}_l = \mathbf{I}, \forall l \\ \mathbf{C}_k^H \mathbf{C}_k = \mathbf{I}, \forall k}} \sum_{k=1}^{K} \sum_{\substack{j=1 \\ j \neq k}}^{K} \mathrm{Tr}\left(\boldsymbol{\Phi}_k^H \left(\mathbf{H}_{kj} \mathbf{V}_j \mathbf{V}_j^H \mathbf{H}_{kj}^H + \mathbf{R}_k\right) \boldsymbol{\Phi}_k\right), \qquad (3.34)$$

where $\boldsymbol{\Phi}_k$ is the orthonormal basis of a subspace orthogonal to the interference subspace, which is generated by interfering transmitters and $\mathbf{R}_k$ is the covariance matrix of the external interference plus noise.

Equation (3.34) can also be minimized through the alternating approach, where the interference subspace and precoders are given by

$$\boldsymbol{\Phi}_k^{opt} = \nu_{min}^{S_k}\left(\sum_{\substack{j=1 \\ j \neq k}}^{K} \mathbf{H}_{kj} \mathbf{V}_j \mathbf{V}_j^H \mathbf{H}_{kj}^H + \mathbf{R}_k\right) \qquad (3.35)$$

and

$$\mathbf{V}_k^{opt} = \nu_{min}^{S_k}\left(\sum_{\substack{j=1 \\ j \neq k}}^{K} \mathbf{H}_{kj}^H \boldsymbol{\Phi}_j \boldsymbol{\Phi}_j^H \mathbf{H}_{kj}\right), \qquad (3.36)$$

where S indicates the "number of streams" such that S_k is the number of streams transmitted by user k and $\nu(\cdot)_{min}^{S_k}$ is a function that returns a matrix whose columns are the eigenvectors corresponding to the S_k smallest eigenvalues of the input matrix.

According to the relationship above, a similar alternating optimization approach can be applied in this case, but now accounting for the external interference suffered by the receivers, as shown in (3.35). The steps of the alternating optimization considering external interference are summarized in Algorithm 3.5.

Note that this alternating approach is only concerned with the interference subspaces and these subspaces should also follow the

external interference directions. Consequently, in some cases, these directions will not provide the optimal solution. The optimal solution would only be achieved if one or more users are sending less streams than they could, i.e., the system is not using all DoF that are available. Furthermore, the external interference arriving in multiple directions can also be considered, but the subspace needs to have the same dimension of this interference, otherwise it will always leak interference in the desired signal space.

Algorithm 3.5 Interference Alignment via Alternating Minimization considering External Interference.

---

i. Fix $\mathbf{V}_l$ arbitrarily for all l;

ii. Let the columns of $\boldsymbol{\Phi}_k$ be the S_k least dominant eigenvectors of $\sum_{k \neq l} \mathbf{H}_{k,l} \mathbf{V}_l \mathbf{V}_l^H \mathbf{H}_{k,l}^H + \mathbf{R}_k$;

iii. Let the columns of $\mathbf{V}_l$ be the S_l least dominant eigenvectors of $\sum_{l \neq k} \mathbf{H}_{k,l}^H \boldsymbol{\Phi}_k \boldsymbol{\Phi}_k^H \mathbf{H}_{k,l} \quad \forall l$;

iv. Repeat steps 2 and 3 until convergence.

3.2.5 Initialization of the Precoding Matrices

Some of the algorithms presented in the previous sections can suffer from a drawback concerning their initialization methods, which are based on a random selection. Alternative initialization methods are presented in [48], which are described below. Three initialization methods are as follows:

i. Right singular matrices initialization:

Initialize $\mathbf{v}_k$ as the first $\mathbf{D}_k$ columns of right singular matrix of the channel coefficient matrix $\mathbf{H}_{kk}$. Then normalize $\mathbf{v}_k$ to satisfy the power constraint of the transmitter k.

ii. Explicit IA solutions initialization:

According to [12], the explicit IA solutions are achieved. Then they are normalized to satisfy the power constraint of each transmitter. This initialization method is only available in certain cases.

iii. Random matrices initialization:

Random matrices are generated according to normal distribution with zero mean and unit variance. They may be normalized to satisfy the power constraint of each transmitter.

It is worth mentioning that not all of these methods are properly motivated. We do consider that there is some room for exploring and proposing other initialization methods for improving IA performance.

3.3 Limitations of IA

The analyses of IA have focused on the case in which global channel knowledge is available at each node of the network because one of the main limitations in order to perform IA is the requirement of CSI at the transmitter. Several distributed algorithms have been proposed since then, with the difference that only local CSI is required. Hence, more studies about the impact of limited feedback on IA are necessary.

Furthermore, the theory of IA was derived under assumptions regarding the richness of the propagation channel, while in practice most channels do not guarantee such ideal decorrelation [54]. Also, even the most fundamental aspect in the analysis of interference alignment schemes, the number of DoF, is only known for some cases. Closed-form interference alignment solutions, assuming constant-coefficient channels, are difficult to derive for more than three users [53]. Note that even though these limitations may restrict the application of IA, we show in Chapter 5 that significant gains are achievable in those cases in which alignment is actually feasible.

3.4 Remarks and Conclusions

In this chapter we presented the closed-form solution for three-user MIMO. According to elapse this work, the used approach is most usual despite of we know that existing other closed-form solutions. When the closed-form solution is difficult to obtain, another way is taking advantage of the IA algorithms. Therefore, we present some IA algorithms belonging to centralized and distributed classes.

Finally, we disseminate the accessible information on the literature about the initialization of the precoders and the limitations of interference alignment.

Chapter 4

Scheduling Strategies

In the literature two strategies employ additional DoF to improve diversity: antenna selection and multiuser diversity. In [21] Klotz and Sezgin investigate the combination of IA and antenna selection techniques using several metrics to determine the most appropriate measure. Aiming to achieve the gains of Dirty Paper Coding (DPC) with significantly reduced amount of feedback information, Lee and Choi in [22] were motivated by opportunistic beamforming and proposed a practical IA based on an opportunistic user selection in a limited feedback environment.

The basic principle is to serve a subset in which antenna or user is approximately orthogonal to the others to facilitate the separation of the desired signal from the others in its respective receiver. Usually these two techniques are used individually, but an alternative is to use all available resources to determine the basis vectors of precoding matrices which make the desired signal space and the interference signal space roughly orthogonal to each other. Hence, we can try to find an appropriate metric which allows to increase the subspace distance for maximizing the capacity of the system.

In this work, we analyze the use of joint antenna and user selection schemes in order to improve IA performance. Moreover, we evaluate the contribution when the Fubini-Study distance is used as metric, since we were motivated by its application for codebook selection in [34].

4.1 Antenna Selection (AS)

According to Klotz and Sezgin in [21], antenna selection is a powerful method in order to reduce the complexity of transmission and reception

in a multi-antenna system. We evaluate the impact of different antenna selection criteria on the performance of wireless networks using IA, in order to achieve performance improvements. A greedy low complexity selection algorithm is used to avoid the exhaustive search of all possible antenna combinations. The selection criteria we consider for the analysis are based on the properties of the channel, such as eigenvalues of the effective channel matrices, Fubini-Study and chordal distances.

Next, we present the selection criteria used for the simulation results and the greedy algorithms for antenna selection.

4.1.1 AS based on Distance Metrics

The Grassmann manifold $\mathcal{G}_{N,M}(\mathbb{C})$ is the set of all M-dimensional subspaces through the origin in the N-dimensional space $\mathbb{C}^N$. If we assume that two interference signals span the spaces $\mathcal{A}$ and $\mathcal{B}$, respectively, the spaces also belong to the Grassmann manifold such that $\mathcal{A}, \mathcal{B} \in \mathcal{G}_{N,M}(\mathbb{C})$. If we denote the generator matrices of two spaces $\mathcal{A}$ and $\mathcal{B}$ by $\mathbf{A} \in \mathbb{C}^{N \times M}$ and $\mathbf{B} \in \mathbb{C}^{N \times M}$, respectively, M columns of $\mathbf{A}$ and $\mathbf{B}$ are orthonormal, respectively, such as $\mathbf{A}^H \mathbf{A} = \mathbf{I}_M$ and $\mathbf{B}^H \mathbf{B} = \mathbf{I}_M$, and span the spaces $\mathcal{A}$ and $\mathcal{B}$.

The principal angles $\theta_1, \ldots, \theta_n \in [0, \pi/2]$ between $\mathcal{A}$ and $\mathcal{B}$ are defined by [55]

$$\cos(\theta_i) = \max_{u \in \mathcal{A}} \max_{v \in \mathcal{B}} u \cdot v = u_i \cdot v_i. \tag{4.1}$$

On the Grassmannian manifold various distances can be defined. According to Conway in [55], the geodesic distance on $\mathcal{G}_{N_R,M}(\mathbb{C})$ between $\mathcal{A}$ and $\mathcal{B}$ is

$$d_g(\mathbf{A}, \mathbf{B}) = \sqrt{\theta_1^2 + \cdots + \theta_n^2}. \tag{4.2}$$

However, this definition has one drawback: it is not everywhere differentiable.

Lately, the Fubini-Study d_{fs} and chordal distances d_{cd} have been applied to spatially multiplexed MIMO wireless communication systems [56]. These distance metrics are the consequence of wireless system optimization.

The Fubini-Study distance between two matrices $\mathbf{A}$ and $\mathbf{B}$ is [34]

$$d_{fs}(\mathbf{A}, \mathbf{B}) = \arccos |\det(\mathbb{O}(\mathbf{A})^H \mathbb{O}(\mathbf{B}))|, \tag{4.3}$$

while the chordal distance between two matrices **A** and **B** is defined as [21]

$$d_{cd}(\mathbf{A}, \mathbf{B}) = \frac{1}{\sqrt{2}} ||\mathbb{O}(\mathbf{A})\mathbb{O}(\mathbf{A})^H - \mathbb{O}(\mathbf{B})\mathbb{O}(\mathbf{B})^H||_F, \qquad (4.4)$$

where $\mathbb{O}(\mathbf{A})$ is defined as a matrix which consists of the orthonormal basis vectors that span the column space of **A** and $|| \cdot ||_F$ denotes the Frobenius norm.

An alternative form for the chordal distance is defined as [57]

$$d_{cd}(\mathbf{A}, \mathbf{B}) = \sqrt{\sum_{j=1}^{N} \sin^2(\theta_j)}, \qquad (4.5)$$

where θ_j is the principal angle between the two subspaces spanned by the rows of the matrices **A** and **B**. Another form for the chordal distance can be deduced as [22]

$$d_{cd}(\mathbf{A}, \mathbf{B}) = \sqrt{M - \mathrm{Tr}(\mathbb{O}(\mathbf{A})^H \mathbb{O}(\mathbf{B}) \mathbb{O}(\mathbf{B})^H \mathbb{O}(\mathbf{A}))}, \qquad (4.6)$$

where $\mathbb{O}(\mathbf{A})$ and $\mathbb{O}(\mathbf{B})$ can be found via QR decomposition.

Each of these distances corresponds to different ideas of distance between subspaces. Maximizing the chordal distance corresponds to minimizing the sum of the eigenvalues of $\mathbb{O}(\mathbf{A})^H \mathbb{O}(\mathbf{B}) \mathbb{O}(\mathbf{B})^H \mathbb{O}(\mathbf{A})$. The projection two-norm distance is maximized by minimizing the smallest singular value of $\mathbb{O}(\mathbf{A})^H \mathbb{O}(\mathbf{B}) \mathbb{O}(\mathbf{B})^H \mathbb{O}(\mathbf{A})$, while the Fubini-Study distance is maximized by minimizing the product of the singular values of $\mathbb{O}(\mathbf{A})^H \mathbb{O}(\mathbf{B}) \mathbb{O}(\mathbf{B})^H \mathbb{O}(\mathbf{A})$ [34].

The total chordal distance for the three user interference channel is defined as [21]

$$d_{cd,total} = d_{cd}(\mathbf{H}_{11}^{\psi_{k_1}^1}\mathbf{V}_1, \mathbf{H}_{12}^{\psi_{k_1}^1}\mathbf{V}_2) + d_{cd}(\mathbf{H}_{22}^{\psi_{k_2}^2}\mathbf{V}_2, \mathbf{H}_{21}^{\psi_{k_2}^2}\mathbf{V}_1) + d_{cd}(\mathbf{H}_{33}^{\psi_{k_3}^3}\mathbf{V}_3, \mathbf{H}_{31}^{\psi_{k_3}^3}\mathbf{V}_1),$$
$$(4.7)$$

where $\mathbf{H}_{rt}^{\psi_{k_r}^r}$ denotes the channel matrices containing the coefficients of the specific set of selected antennas available between the transmitter t and receiver r.

For the other case, the total Fubini-Study distance for the three user

interference channel is defined as [21]

$$d_{cd,total} = d_{fs}(\mathbf{H}_{11}^{\psi_{k_1}^1}\mathbf{V}_1, \mathbf{H}_{12}^{\psi_{k_1}^1}\mathbf{V}_2) + d_{fs}(\mathbf{H}_{22}^{\psi_{k_2}^2}\mathbf{V}_2, \mathbf{H}_{21}^{\psi_{k_2}^2}\mathbf{V}_1) + d_{fs}(\mathbf{H}_{33}^{\psi_{k_3}^3}\mathbf{V}_3, \mathbf{H}_{31}^{\psi_{k_3}^3}\mathbf{V}_1).$$

(4.8)

Now, we define the effective channel of receiver r as

$$\mathbf{H}_r^{eff,\chi} = \begin{bmatrix} \mathbf{H}_{r1}^{\psi_{k_r}^r}\mathbf{V}_1 & \mathbf{H}_{r2}^{\psi_{k_r}^r}\mathbf{V}_2 & \mathbf{H}_{r3}^{\psi_{k_r}^r}\mathbf{V}_3 \end{bmatrix},$$

(4.9)

where $\chi = \{k_1, k_2, k_3\}$ is the set of indices selecting the antenna subsets at the nodes. Considering a three user MIMO IC, we can rewrite (2.29) as

$$\mathbf{y}_r = \mathbf{H}_r^{eff,\chi} \begin{bmatrix} \mathbf{x}_1 \\ \mathbf{x}_2 \\ \mathbf{x}_3 \end{bmatrix} + \mathbf{n}_r = \mathbf{H}_r^{eff,\chi}\mathbf{x} + \mathbf{n}_r.$$

(4.10)

where, $\mathbf{x}_t$ represents the messages at the transmitter t. In order to retrieve the corresponding transmitted signal, we can multiply (4.10) by the Moore-Penrose pseudo-inverse $\mathbf{H}_r^{eff,\chi}$ of the effective channel. For the first receiver we can get

$$\hat{\mathbf{x}} = \left(\mathbf{H}_1^{eff,\chi}\right)^\dagger \mathbf{y}_r$$

$$= \left(\mathbf{H}_1^{eff,\chi}\right)^\dagger \mathbf{H}_r^{eff,\chi} \begin{bmatrix} \mathbf{x}_1 \\ \mathbf{x}_2 \\ \mathbf{x}_3 \end{bmatrix} + \left(\mathbf{H}_1^{eff,\chi}\right)^\dagger \mathbf{n}_r$$

$$= \begin{bmatrix} \mathbf{I}_{N/2} & \mathbf{0}_{N/2} & & \mathbf{0}_{N/2} \\ \mathbf{0}_{N/2} & & & \\ & & \mathbf{U} & \\ \mathbf{0}_{N/2} & & & \end{bmatrix} \begin{bmatrix} \mathbf{x}_1 \\ \mathbf{x}_2 \\ \mathbf{x}_3 \end{bmatrix} + \left(\mathbf{H}_1^{eff,\chi}\right)^\dagger \mathbf{n}_r,$$

(4.11)

where $\mathbf{I}_{N/2}$ and $\mathbf{0}_{N/2}$ are an $N/2 \times N/2$ identity matrix and an all zero matrix, respectively. The matrix $\mathbf{U}$ is rank deficient, i.e., $\mathrm{rank}(\mathbf{U}) = 1$ and depends on the channel gains. Let us denote by $[\mathbf{A}]_k$ a matrix consisting of the $N/2$ rows between row $kN/2 + 1$ and row $(k + 1)N/2 + 1$ of the matrix $\mathbf{A}$. Then,

in general the desired signal at the rth receiver can be written as

$$\hat{\mathbf{x}}_r = \mathbf{x}_r + \left(\mathbf{H}_r^{eff,\chi}\right)^\dagger \mathbf{n}_r. \tag{4.12}$$

Thus, the sum rate can be written as

$$R_{\sum}(\chi) = \sum_{r=1}^{3} \log_2 \det \left(\mathbf{I} + \frac{P}{N_0}\left(\left[\left(\mathbf{H}_1^{eff,\chi}\right)^\dagger\right]_r \left[\left(\mathbf{H}_1^{eff,\chi}\right)^\dagger\right]_r^H\right)^{-1}\right). \tag{4.13}$$

The optimal antenna selection regarding the sum rate, $R_{\sum}$, can be achieved through an exhaustive search over all possible antenna selections. The antenna selection that reaches the optimal sum rate can be achieved by maximizing $R_{\sum}$ such as

$$\chi_{opt} = \arg\max_{\chi} R_{\sum}(\chi), \tag{4.14}$$

where χ is the set of indexes selecting the antenna subsets at the nodes.

The subset which results in the maximum chordal distance $d_{cd,total}$ and its corresponding rate are given by [21]

$$\chi_{cd} = \arg\max_{\chi} d_{cd,total}(\chi), \tag{4.15}$$

$$R_{\sum,cd} = R_{\sum}(\chi_{cd}) \le R_{\sum}(\chi_{opt}). \tag{4.16}$$

The main contribution of this analysis is the use of the Fubini-Study distance as selection criterion, since in the literature only the chordal distance was tested. Then, similarly to the chordal distance case, the subset which results in the maximum Fubini-Study distance is given by

$$\chi_{fs} = \arg\max_{\chi} d_{fs,total}(\chi). \tag{4.17}$$

The greedy algorithm based on chordal distance is presented in [21]. The idea is to start with some initial antenna selection χ_0, and then iteratively change the selection sets at the users in a way that the chordal distance is improved. Next, Algorithm 4.1 presents the main antenna selection steps using either the chordal or the Fubini-Study distance considering the three-user case.

Algorithm 4.1 Greedy Algorithm based on Fubini-Study or Chordal Distances.

1: Initialize maximal distance to zero: $d_{\max} = 0$;
2: **for** $l = 1$ to 3 **do**
3:    **for** $m = 1$ to $\binom{M}{N}$ **do**
4:       Pick the next antenna set at transmitter l:$k_l = k_l + 1$
5:       Update χ
6:       Calculate precoding matrices using (3.4)-(3.6)
7:       Calculate $d(\chi)$: Fubini-Study or chordal distance according to (4.3) or (4.4)
8:       **if** $d(\chi) > d_{\max}$ **then**
9:          Update stored antenna selection $k_l \to \hat{k}_l$
10:          Store maximal Fubini-Study distance $d(\chi) \to d_{\max}$
11:       **end if**
12:    **end for**
13:    Restore best antenna selection: $k_l \leftarrow \hat{k}_l$
14:    Update χ
15: **end for**
16: χ contains the resulting antenna selection

4.1.2 AS based on Eigenvalues of the Effective Channel Matrix

According to (4.18), the SNR mainly depends on the effective channel matrices $\mathbf{H}^r_{eff,\chi}$ and hence on its eigenvalues. Its mathematical formulation is given by

$$SNR_r(\chi) = \frac{P}{N_0 \cdot \text{Tr}\left(\left[\mathbf{H}^{eff,\chi\dagger}_r\right]^H_r \left[\mathbf{H}^{eff,\chi\dagger}_r\right]_r\right)} \tag{4.18}$$

where $\mathbf{H}^{eff,\chi}_r = \left[\mathbf{H}^{\psi^r_{k_r}}_{r1}\mathbf{V}_1\ \mathbf{H}^{\psi^r_{k_r}}_{r2}\mathbf{V}_2\ \mathbf{H}^{\psi^r_{k_r}}_{r3}\mathbf{V}_3\right]$ and $[\cdot]^\dagger$ is the Moore-Penrose pseudo-inverse. Then, the metric based on the eigenvalues can be written as

$$\lambda^\chi = \lambda_1^{\chi^{-1}} + \lambda_2^{\chi^{-1}} + \lambda_3^{\chi^{-1}}, \tag{4.19}$$

where λ_r^χ is the smallest eigenvalue of $H^{eff,\chi}_r$ for receiver r.

The antenna selection is now based on the minimum of λ_χ

$$\chi_{eig} = \arg\min_\chi \lambda^\chi, \tag{4.20}$$

resulting in the sum rate

$$R_{\sum,eig} = R_{\sum}(\chi_{eig}). \tag{4.21}$$

The greedy algorithm based on eigenvalues of the effective channel is presented in [21]. Then, the antenna selection strategy is summarized in Algorithm 4.2.

Algorithm 4.2 Greedy Algorithm based on Eigenvalues of $\mathbf{H}^{eff}$.

1: Initialize maximal eigenvalue metric: λ_{min};
2: **for** $l = 1$ to 3 **do**
3:    **for** $m = 1$ to $\binom{M}{N}$ **do**
4:       Pick the next antenna set at transmitter l: $k_l = k_l + 1$
5:       Update χ
6:       Calculate effective matrices $\mathbf{H}_r^{eff,\chi}$, $r \in (1,2,3)$
7:       Calculate sum of inverse eigenvalues λ^χ according to (4.19)
8:       **if** $\lambda^\chi < \lambda_{\min}$ **then**
9:          Update stored antenna selection $k_l \to \hat{k}_l(i_l \to \hat{i}_l)$
10:          Store minimal eigenvalue $\lambda^\chi \to \lambda_{\min}$
11:       **end if**
12:    **end for**
13:    Restore best antenna selection: $k_l \leftarrow \hat{k}_l$
14:    Update χ
15: **end for**
16: χ contains the resulting antenna selection

4.2 User Selection

In multiuser scenarios, the number of simultaneous users that can be served is limited by the number of transmit and receive antennas. As the number of users K increases, the probability of finding users with good channel conditions increases as well, so that the best subset of users can be chosen in order to maximize the throughput. This form of selection diversity is called multiuser diversity [57]. Due to the high complexity of exhaustive search, several suboptimal user selection algorithms were studied in [58, 59].

The basic idea is to select a set of users in which each one is approximately orthogonal to the others by using a user selection algorithm based on chordal distance. At each step, the user whose channel matrix has the largest chordal distance with the matrix spanned by the channels of the previously selected users is selected.

The system model in this case is depicted in Figure 4.1. There are three transmitters and each transmitter has its own user group. Each transmitter has M antennas and each user group consists of K receivers having N antennas each. Since only a single user in each group is selected and served by each transmitter, the transmitters and the selected users build up a three-user MIMO IC.
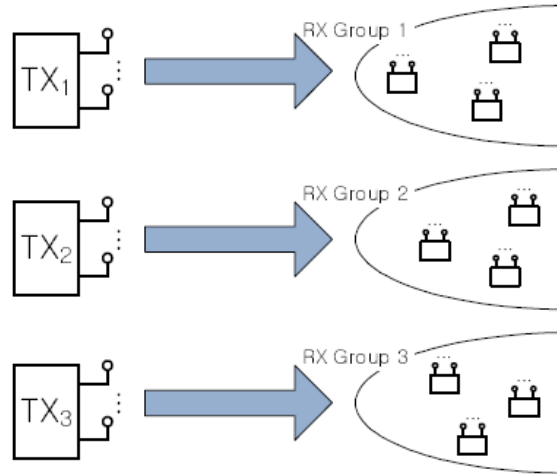

Figure 4.1 – System model[1]. Each transmitter selects one user in each group.

In this scenario we consider a different approach for performing the precoding, which is now based on random beamforming in order to take advantage of the available multiuser diversity. The transmission at each transmitter takes four steps as follows.

i. Step 1: The ith transmitter sends a random broadcast beam;

ii. Step 2: Each receiver feeds back its value of distance to its respective transmitter;

iii. Step 3: Each transmitter selects a single user in its own group according to the user selection criterion;

iv. Step 4: Finally, the selected user is served with the beam generated by zero-forcing method.

In the first step, the ith transmitter broadcasts the signal using a random beamforming matrix. Then, in the second step, each user feeds

---

[1]This figure was drawn from [22].

back one analog value to the transmitter to which the user belongs. In the third step, each transmitter selects a single user in its own user group according to the information fed back from users. Finally, after user selection at each transmitter, in the fourth step the selected user is served with the random beams.

Since the kth user in the first user group has two interference channels $\mathbf{H}_{12}^{[k]}$ and $\mathbf{H}_{13}^{[k]}$, the transmitter selects the user whose measure of interference alignment is minimum such as

$$k_1 = \arg\min_{1<k'<K} d_{cd}^2(\mathbf{H}_{12}^{[k']}\mathbf{V}_2, \mathbf{H}_{13}^{[k']}\mathbf{V}_3). \tag{4.22}$$

Similarly to the antenna selection case, the main purpose of this analysis was to compare different selection criteria, with the addition of the Fubini-Study distance, which was not employed so far in such case. Then, similarly to the procedure of chordal distance, the transmitter now selects the user with minimum Fubini-Study distance:

$$k_1 = \arg\min_{1<k'<K} d_{fs}^2(\mathbf{H}_{12}^{[k']}\mathbf{V}_2, \mathbf{H}_{13}^{[k']}\mathbf{V}_3). \tag{4.23}$$

4.3 Remarks and Conclusions

With regard to the antenna selection and user selection studies, different selection criteria were studied using the greedy algorithms. An important question is how best to determine the number of necessary antennas and/or users for these considered metrics with interference alignment in mind. A possible next step is to investigate schemes based on Fubini-Study and chordal distances which allow to use simultaneously the antenna selection and multiuser selection, with the purpose of improving the interference alignment at the intended receivers.

Chapter 5

Simulation Results

In order to compare the performances of the interference alignment systems presented in the previous sections, this chapter presents the obtained simulation results.

At first, we define some scenarios and parameters for computer simulations. These scenarios are proposed in order to allow the analysis of the IA algorithms behavior in the K-user $M \times N$ MIMO IC system model.

The IA algorithms considered are the ZF, MMSE, pricing and alternating presented previously. We analyzed an alternative utility function for pricing algorithm in relation to the sum rate and fairness of the resources. Then, we investigate the impact of the transmit antenna correlation, CSI and external interference on the algorithms.

In search of other possible approaches, which can improve the robustness of IA and provide additional DoF, we explore the antenna and user selection strategies and we propose a joint antenna and user selection. Moreover, beyond the traditional metrics, we evaluate the performance of the IA algorithm using the Fubini-Study distance.

5.1 Simulation Scenarios and Parameters

In this section, we present the proposed simulation scenarios and parameters used to generate the results. We describe two different scenarios: one where users are far from the cell center and illustrated in Figure 5.1(a), and another where users are close to the cell center and illustrated in Figure 5.1(b). In both scenarios the users are located at positions corresponding to 70% of the distance from the cell center to the border and the SNR value indicated in each figure caption corresponds to the average SNR the user would see at the border of the cell.

(a) Users far from the cluster center.

(b) Users close to the cluster center.
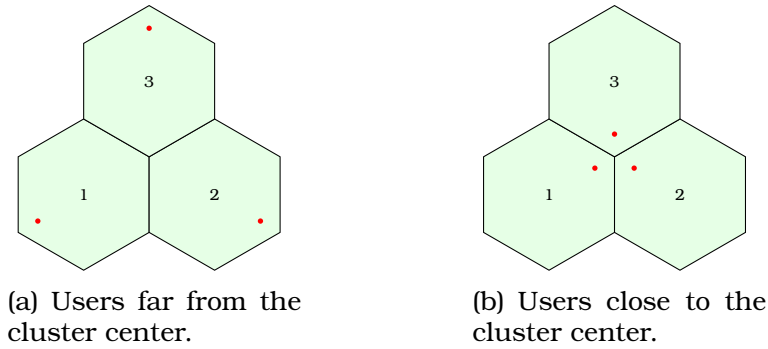
Figure 5.1 – Cluster with three cells with one mobile at each cell.

The simulation parameters are summarized in Table 5.1. The SNR values we refer are related to the average SNR the user sees at the border of the cell, since the transmission power of each base station is calculated to match this signal quality at the border.

Table 5.1 – Simulation Parameters.

Parameter	Value
Cell Radius	1 km
Antennas (each Base)	2
Antennas (each user)	2
Modulation	4-PSK
Path Loss Model (in dB with d in km)	$128.1 + 37.6 \log_{10}(d)$
Noise Power	$N_0 =$ -116.4 dBm
Transmission Power	Changed to match SNR at the border of the cell

5.2 Simulation Results for Pricing Algorithm

In this section, we evaluate the simulation results for sum rate utility and "α-fair" utility functions in the optimization problem presented in (3.21). We consider a three-user system with two transmit and two receive antennas for each user. The direct channel and cross channel matrices have i.i.d complex Gaussian entries with unit variance, that is, the direct and interference channel matrices have elements with only Rayleigh fading.

In Figure 5.2, we show the sum rate performance versus SNR, averaged over 500 channel realizations, for different values of α. We observe the impact of α in the trade-off between the egoistic (first term in (3.21)) and altruistic objectives (second term in (3.21)) yielding different sum rate values.
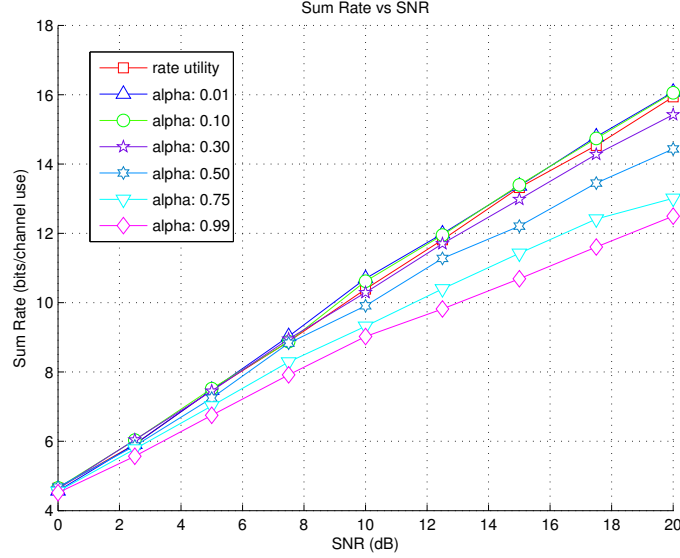
Figure 5.2 – Illustration of the performance of rate utility and "α-fair" utility functions in the distributed pricing algorithm.

In order to draw some insights about the impact of changing the α parameter in the pricing algorithm, let's consider the egoistic and altruistic parts in (3.21). The egoistic part can be written as

$$f_k(\gamma_k) = \frac{\gamma_k^{\alpha}}{\alpha} = \frac{S_k{}^{\alpha}}{\alpha(I_k + N_k)^{\alpha}} \tag{5.1}$$

and the altruistic part can be written as

$$\sum_{j \neq k} \pi_j |\mathbf{u}_j^H \mathbf{H}_{jk} \mathbf{v}_k|^2 = \sum_{j \neq k} \pi_j L_{jk} = \sum_{j \neq k} \frac{S_j{}^{\alpha}}{(I_j + N_j)^{\alpha+1}} L_{jk}, \tag{5.2}$$

where L_{jk} is a constant (we are interested in the variation with alpha). Because both terms vary differently with alpha, then changing α will change the relation between the egoistic and altruistic objectives.

However, determining the optimal value of α is a difficult problem. An empirical value of α can be obtained from Figure 5.2 by choosing the value that yields the highest sum rate. The numerical results show that for low

values of α (0.10 or lower) the α-fair function achieves better performance than the rate utility function. In order to analyze how this gain is spread among the users, the Cumulative Distribution Functions (CDFs) of the worst and best obtained rates are shown, respectively, in Figures 5.3 and 5.4.
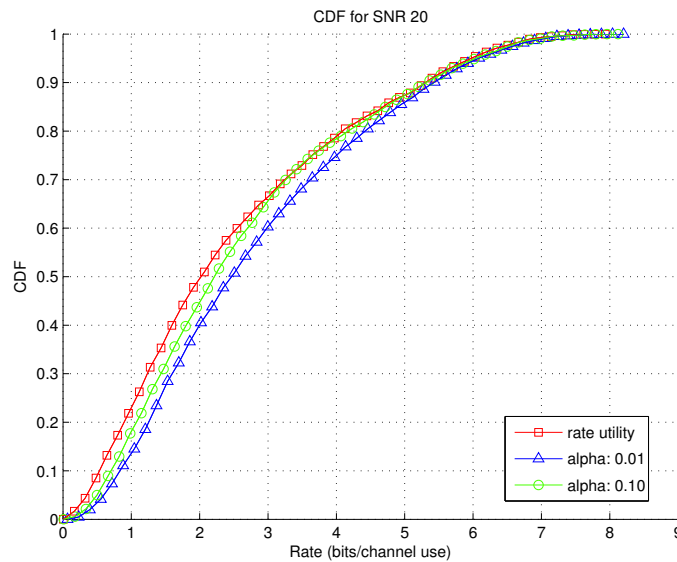
Figure 5.3 – Illustration of CDF of the worst rate.
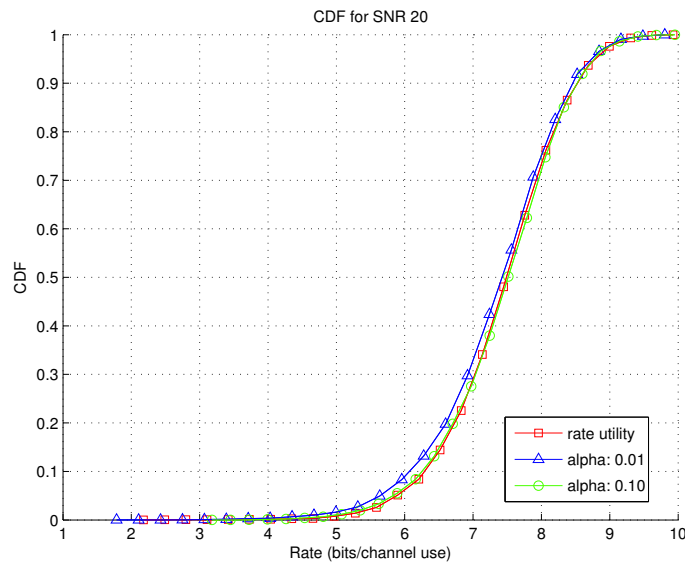
Figure 5.4 – Illustration of CDF of the best rate.

In Figure 5.3 we see that the worst obtained rate is better comparing to the obtained rate when using the original rate utility function. On the

other hand, Figure 5.4 shows that the best obtained rate has no gain (or loss), resulting in approximately the same performance as the original rate utility function. That is, although not large, the gain when using the α-fair utility function comparing to the original rate utility goes to the user who needs it the most.

In the next section, we investigate the impact of the transmit antenna correlation and CSI on the remaining algorithms.

5.3 Simulation Results with Imperfect CSI

In this section, we examine the impact of transmit antenna correlation and CSI error generated by (2.28) in the proposed scenarios. According to Table 5.1, both users and Base Stations (BSs) have two antennas while only one stream is transmitted by each user, corresponding to the maximum number of degrees of freedom which can be achieved in that case.

We analyze the effect of transmit antenna correlation (ϕ parameter) and CSI estimation error (β parameter) for the specific scenarios described previously. These effects are considered only at the transmitter in the sum capacity curves. That is, the estimated (correlated) channel is used to perform IA and the Shannon capacity is calculated for the resulting equivalent channel. The main objective is to grasp the effect caused by the choice of the ϕ and β values in the ZF, MMSE and alternating algorithms. Moreover, we must evaluate how they can provide gains or performance loss in relation to the sum capacity and BER metrics.

Figures 5.5(a) and 5.5(b) show the impact of correlation (ϕ) when users are far from the cell center and when users are close to the cell center, respectively. It is possible to analyze the impact of ϕ in the interval $0.2 \leq \phi \leq 0.9$ for an SNR of 0 dB for both scenarios. We verify that the increase of ϕ causes reduction of the sum capacity value of all algorithms presented.

Figures 5.5(c) and 5.5(d) exhibit the results for both scenarios due to the variation of β values in the range $0 \leq \beta \leq 1$. We note that MMSE is more sensitive to channel estimation errors than the other algorithms for low SNR values.

Figure 5.6 shows BER curves as a function of the variation of the ϕ and β parameters. We can see that both correlation and CSI estimation error, as expected, have a negative impact on the sum rate due the increase of

BER. The algorithms maintain their relative order of BER performance throughout the whole range in which the parameters are varied. The best BER performance was achieved by the IA-MMSE algorithm, which was also an expected result, given that the MMSE criterion is better suited to the BER metric. When β is very high all the IA algorithms have practically no useful CSI available at the transmitter and the BER goes to 0.5. However, even for high levels of ϕ some information can still be decoded.
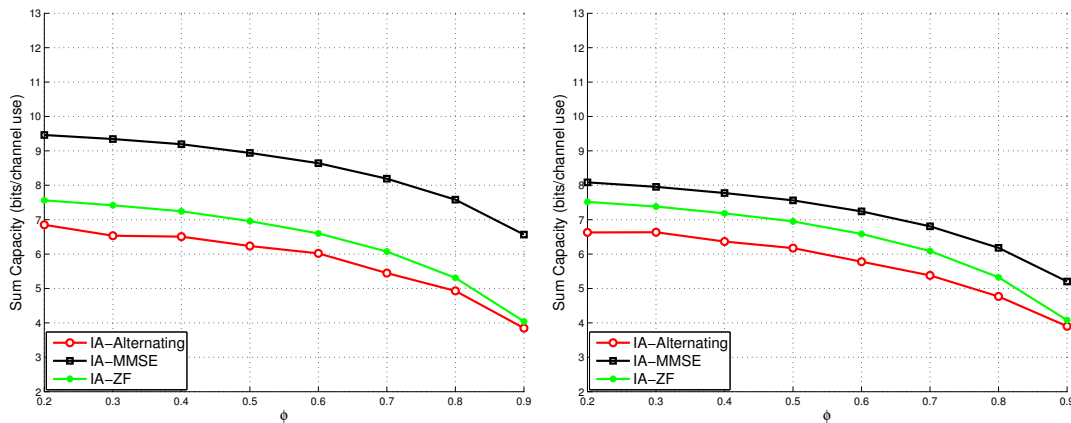
(a) Impact of correlation (ϕ) when users are far from the cell center.
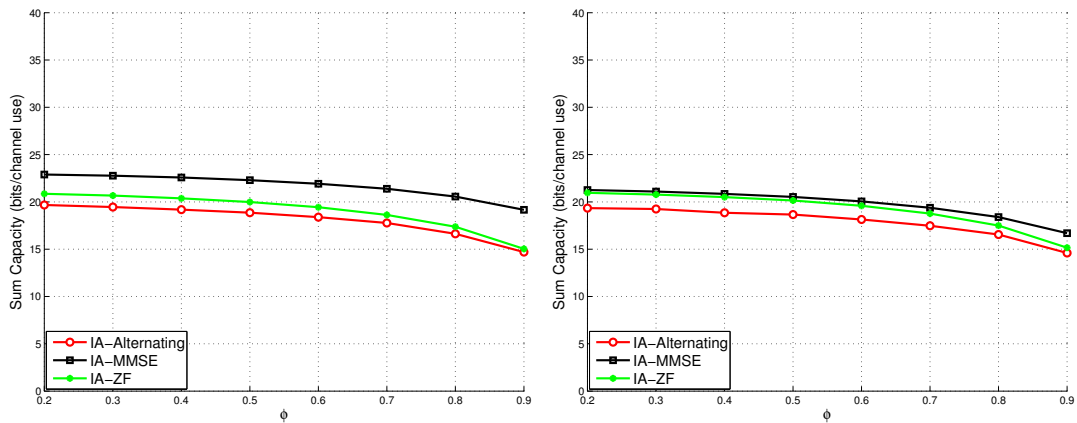
(b) Impact of correlation (ϕ) when users are close to the cell center.
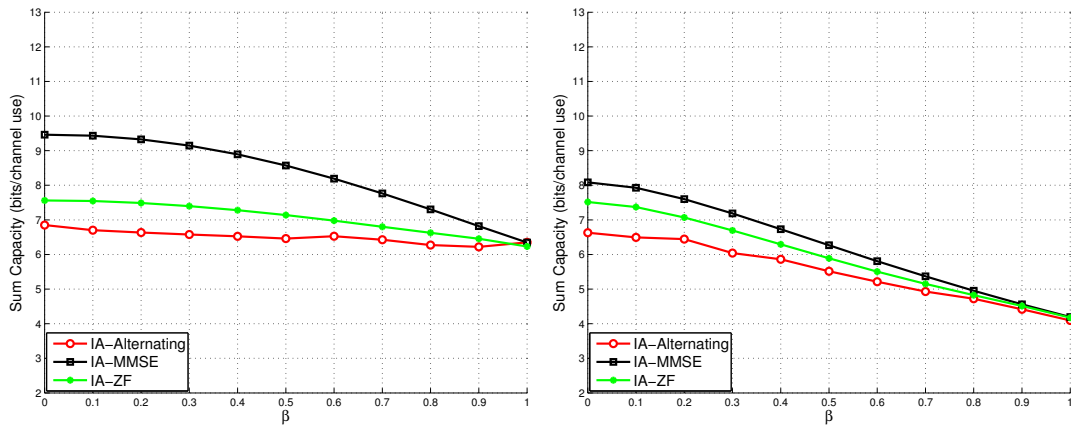
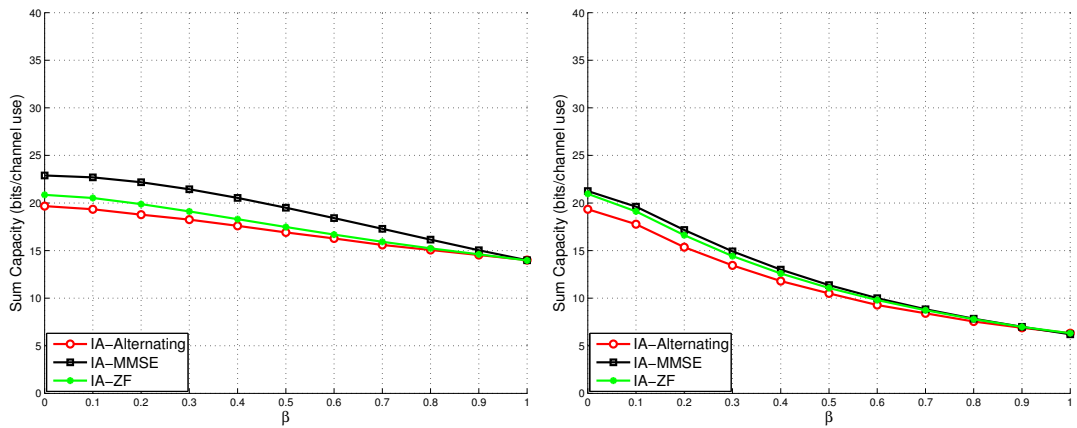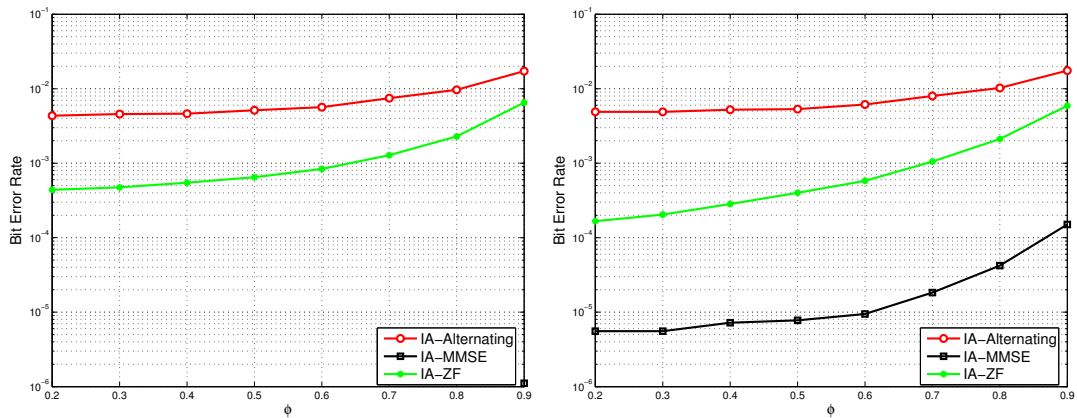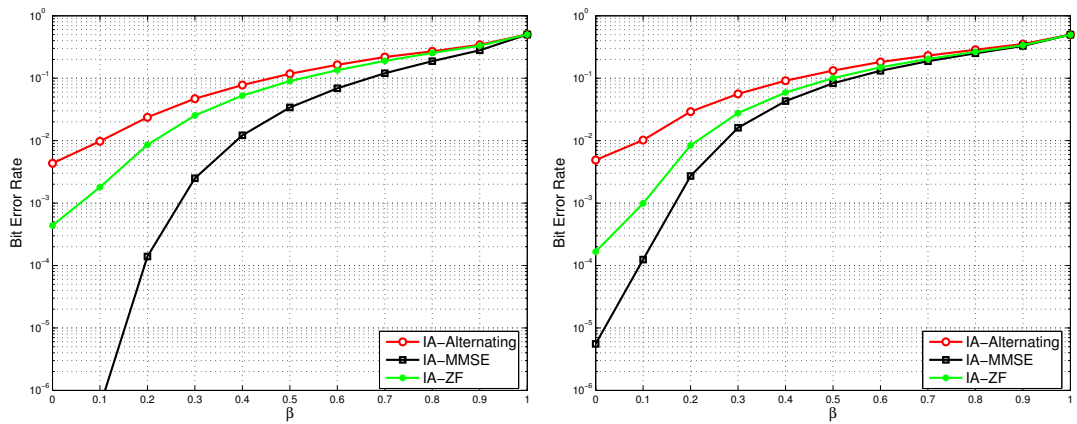(c) Impact of CSI est. error (β) when users are far from the cell center.

(d) Impact of CSI est. error (β) when users are close to the cell center.

Figure 5.5 – Impact of ϕ and β on the sum rate for SNR = 0 dB.

A similar set of results, with both sum capacity and BER measures, is now obtained for an average SNR of 15 dB at the cell border. Figure 5.7 shows the sum capacity results, which now achieve much higher values due to the better channel conditions.

Figure 5.8 shows the BER results for the 15 dB configuration, from which the same conclusions can be drawn as from Figure 5.6, with IA-MMSE presenting a much better BER performance. Note that in Figure 5.8(a) only one point of the IA-MMSE curve is shown, given that lower BER values are achieved than the range displayed in the figure.

Therefore, we conclude that imperfect CSI is more destructive for the IA network than the effect of antenna correlation. Moreover, the MMSE algorithm is more affected than the other algorithms, since it starts much better for low phi and beta values and then steeply deteriorates toward the other algorithms as phi and beta increase.
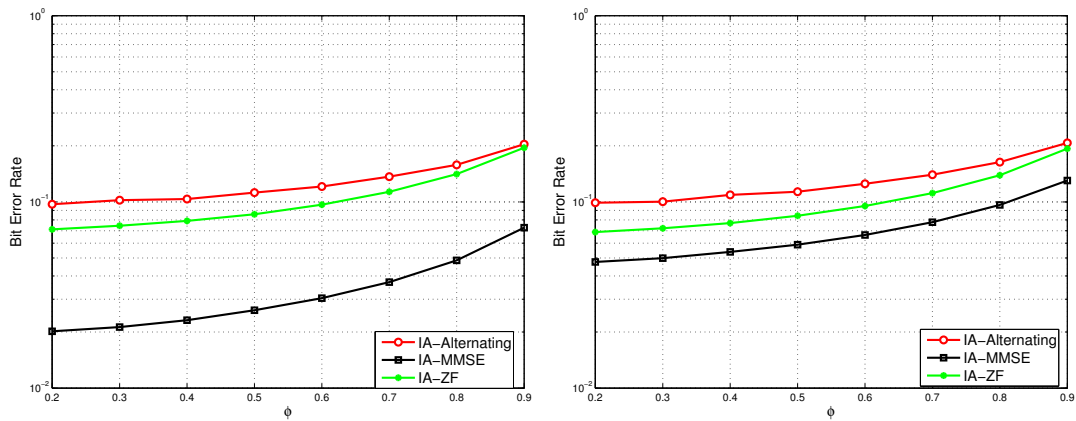
(a) Impact of correlation (ϕ) when users are far from the cell center.

(b) Impact of correlation (ϕ) when users are close to the cell center.
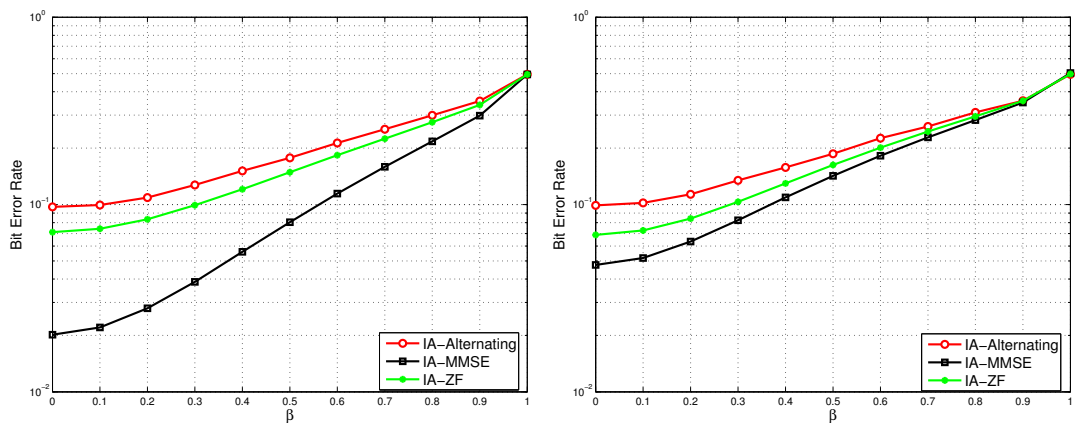
(c) Impact of CSI est. error (β) when users are far from the cell center.

(d) Impact of CSI est. error (β) when users are close to the cell center.

Figure 5.6 – Impact of ϕ and β on the BER for SNR = 0 dB.

(a) Impact of correlation (ϕ) when users are far from the cell center.

(b) Impact of correlation (ϕ) when users are close to the cell center.

(c) Impact of CSI est. error (β) when users are far from the cell center.

(d) Impact of CSI est. error (β) when users are close to the cell center.

Figure 5.7 – Impact of ϕ and β on the sum rate for SNR =15 dB.

(a) Impact of correlation (ϕ) when users are far from the cell center.

(b) Impact of correlation (ϕ) when users are close to the cell center.

(c) Impact of CSI est. error (β) when users are far from the cell center.

(d) Impact of CSI est. error (β) when users are close to the cell center.

Figure 5.8 – Impact of ϕ and β on the BER for SNR =15 dB.

5.4 Simulation Results for Antenna and User Selection

This section presents simulation results of the algorithms described in Sections 4.1.1 and 4.1.2. Continuing with the same scenario and simulation parameters, the additional information in Table 5.1 is the number of available antennas for each base to realize the selection is $M = 3$ while the number of amplifiers and hence the number of antennas that can be used is $N = 2$. The performance of the selection methods is presented by means of numerical results and has been obtained by means of Monte-Carlo simulations. We generated channel matrices following a complex Gaussian distribution with zero mean and variance $\sigma^2 = 1$.

Figure 5.9(a) and 5.9(b), present the sum rate of different methods with IA-ZF, which are depicted when users are far from the cell center and when users are close to the cell center, respectively. We can see that all methods are better than the random antenna selection. In fact, the methods based on the Fubini-Study and chordal distances, as well on the eigenvalues of the effective channel, present a similar (and better than random) performance because they choose a subset of antennas which facilitates the alignment of interference at the intended receiver and thus increase the total capacity of the system.

Then, the chordal and Fubini-Study distances are evaluated and compared for the random user selection scheme. In this scenario, the additional information in Table 5.1 is number D of the available receivers in each group.

For the random user selection scheme, Fig. 5.10 presents the result of the sum rate for a three user MIMO IC with $(M, D, N) = (2, 2, 2)$ utilizing the ZF criterion. In fact, the methods based on the Fubini-Study and chordal distances, as well as on the eigenvalues of the effective channel, present a similar (and better than random) performance because they choose a subset of antennas which facilitates the alignment of interference at the intended receiver and thus increases the total capacity of the system. Note that this is an initial step of the antenna and/or user selection study. Further, analyses are required in order to better understand the trade-offs of the considered metrics.
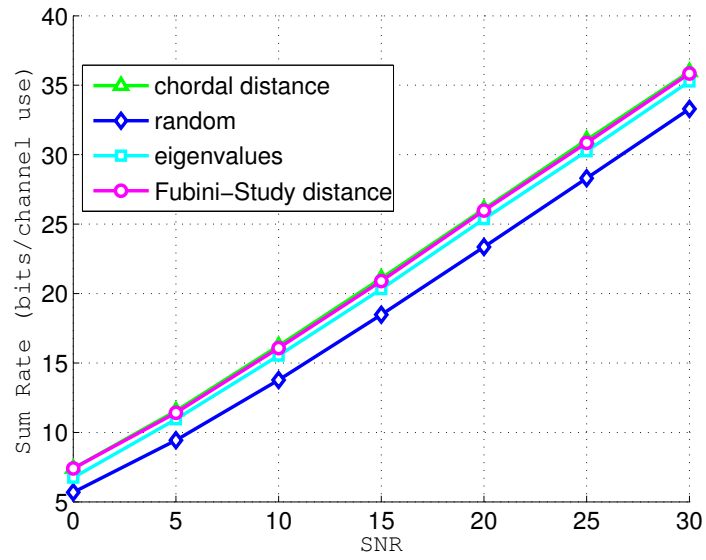
(a) Sum rate of antenna selection when users are far from the cell center.
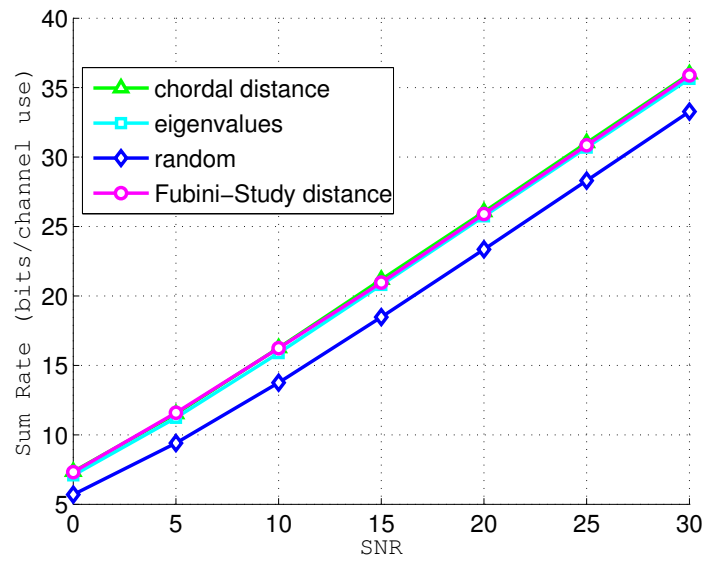
(b) Sum rate of antenna selection when users are close to the cell center.

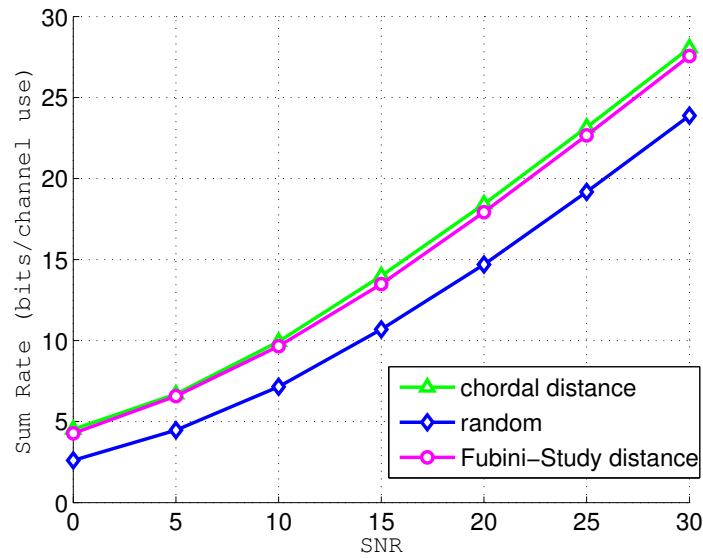Figure 5.9 – Sum rate of greedy antenna selection methods.

Figure 5.10 – Sum rate of user selection methods.

5.5 Simulation Results for Joint Antenna and User Selection

In this section, we propose to use a joint antenna and user selection scheme for IA. We perform the following proposed joint scheme: initially the user selection is applied and then the antenna selection is used to choose at each transmitter the best antennas according to the selection method.
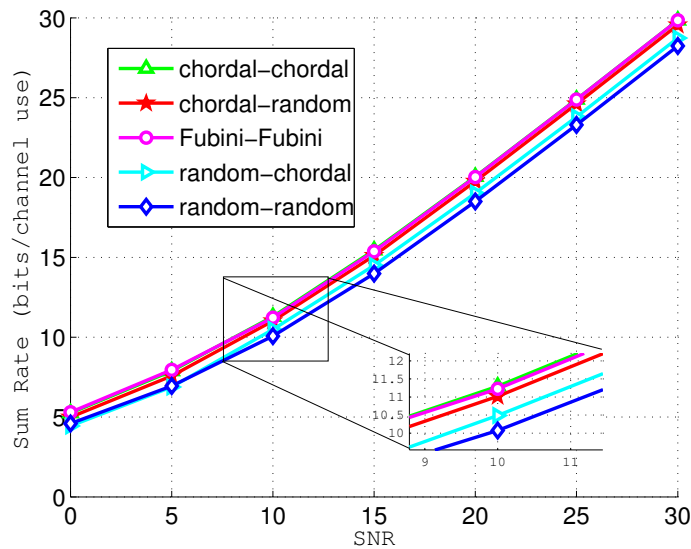
Figure 5.11 – Sum rate of joint antenna and user selection.

In Fig. 5.11, the sum rate of the proposed method is depicted. The legend indicates the criterion used for each selection technique e.g. (antenna;user) = (chordal-chordal) means that the chordal distance was used for both selections. The sum rate when we used the chordal distance criterion presents a similar performance with the Fubini-Study distance criterion. As expected, both sum rate curves obtain a better performance than the random choice.

5.5.1 Simulation Results with CSI

In this section, we investigate the impact of path loss in the choice of joint antenna and user selection considering CSI error. The chosen scenario is the one where users are far from the cell center, and illustrated in Figure 5.1(a) for the value of SNR equal to 15 dB. The imposed variation of user locations is different with regard to the distances of their base stations, which is distributed around the circle generated by the same distance. According to Table 5.1, the additional information is that the number of available antennas for each base to realize the selection is $M = 3$ while the number of amplifiers and hence the number of antennas that can be used is $N = 2$. Only one stream is transmitted by each user, corresponding to the maximum number of degrees of freedom which can be achieved in that case.

Figure 5.12 presents the sum rate of joint antenna and user selection methods with CSI. As noted in the results, the effect of path loss decreases the total sum rate for both used metrics. The consequence is worse values of BER according to Figure 5.13. Due to the limitation of IA which, in order to operate properly, requires the availability of CSI at the transmitter, its performance is severely degraded under adverse conditions.
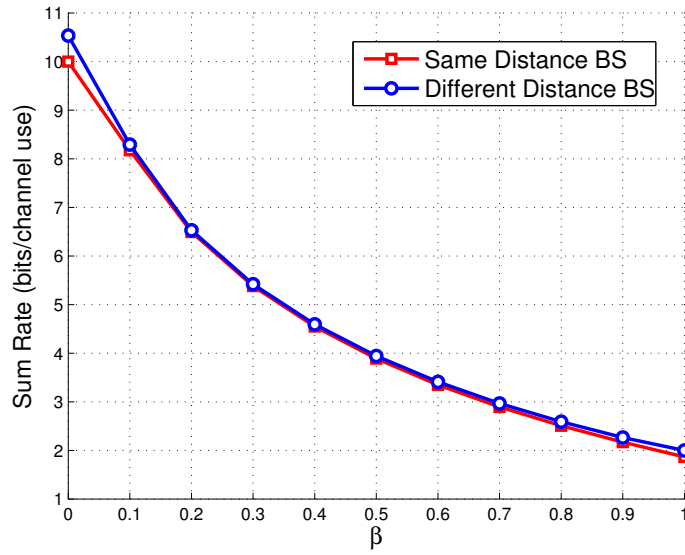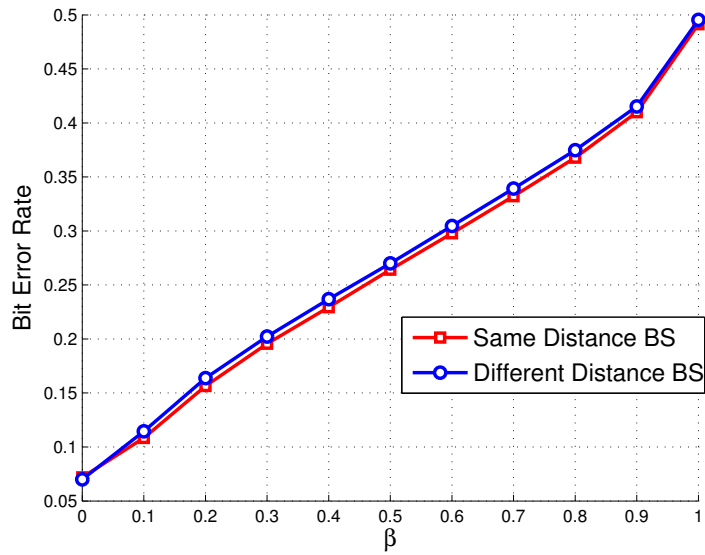
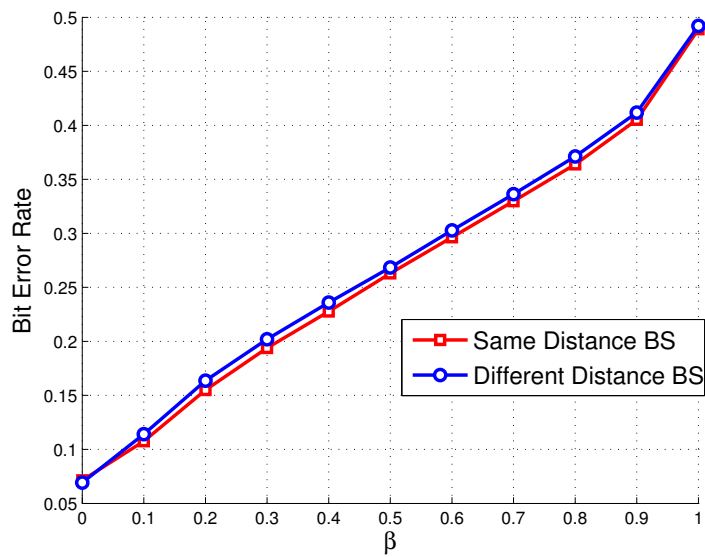(a) Sum rate of joint antenna and user selection with the chordal distance criterion.
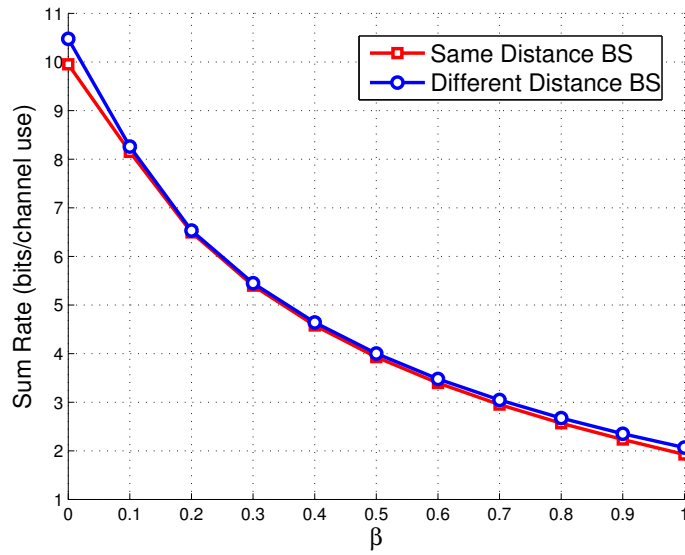
(b) Sum rate of joint antenna and user selection with the Fubini-Study distance criterion.

Figure 5.12 – Sum rate of joint antenna and user selection methods with CSI.

(a) BER of joint antenna and user selection with the chordal distance criterion.

(b) BER of joint antenna and user selection with the Fubini-Study distance criterion.

Figure 5.13 – BER of joint antenna and user selection methods with CSI.

5.6 Simulation Results with External Interference

In this section, we investigate the impact of external interference. In order to evaluate the impact of the external interference on the performance of the algorithms based on the IA approaches, computer simulations were performed in a scenario with only one cluster which is composed by three cells with one user per cell, forming, this way, a three user interference channel shown in Figure 5.14. The performance analyses were based on the average sum capacity and BER, which are able to provide a good insight of the throughput of the system.

(a) Users distributed over all the cluster.

(b) Users distributed close to the border of the cluster, respecting a distance of 1.3 km from the center.
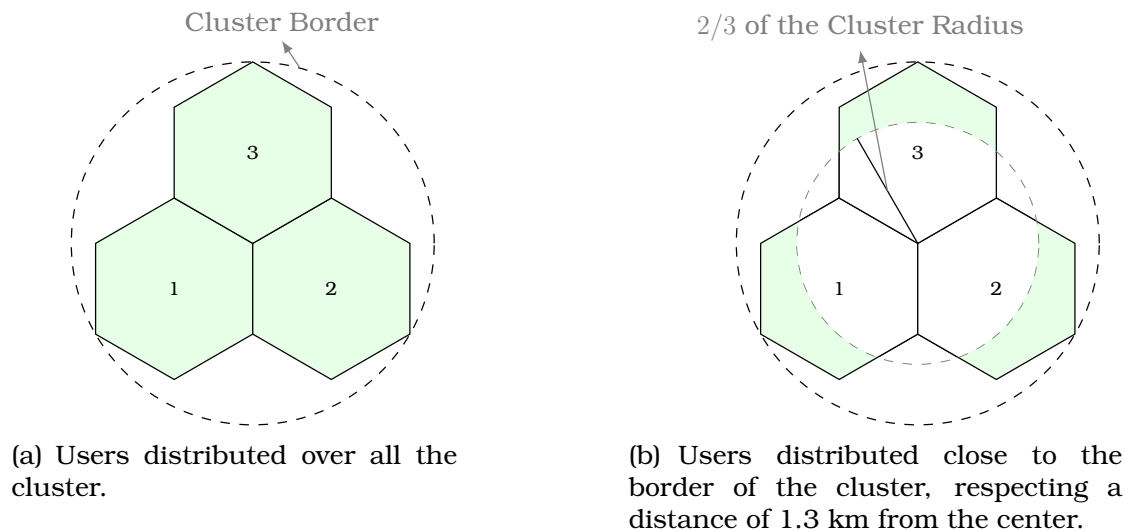
Figure 5.14 – Cluster with three cells with one mobile at each cell.

Some modifications may be observed to the computational simulations. Figure 5.14(a) shows the scenario when the users were distributed randomly over all the cluster. In another situation, users were placed closer to the border of the cluster, respecting a certain distance from the center of the cluster as illustrated in Figure 5.14(b). Since border users experience more interference, this variation at the scenarios is important because it increases the effect of the external interference and it will better reflect the impact of external interference. The additional information in Table 5.1 is the cluster Radius with 2 km.

The external interference for each user was modeled as a colored noise with one dominant direction, which means a highly spatially correlated noise with a rank-one covariance matrix. Therefore, each user perceives a different external interference, with different direction and power, due

to the distinct users location. Consequently, the labels of external interference correspond to the average power of external interference at the border of the cluster. The algorithms that realize a treatment of the external interference are referred as enhanced algorithms with *ext.* after their names in the figure's legend.
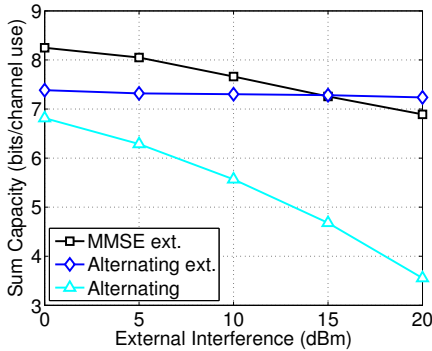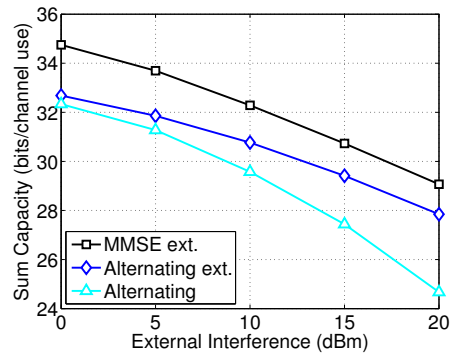

(a) SNR of 0 dB at the border of the cell.
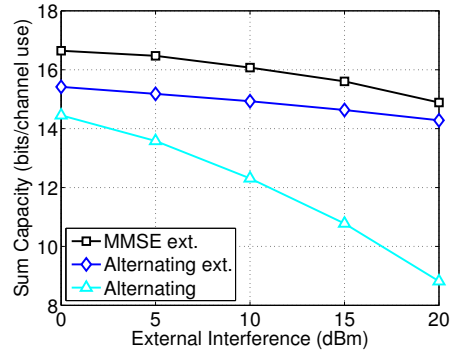
(b) SNR of 10 dB at the border of the cell.
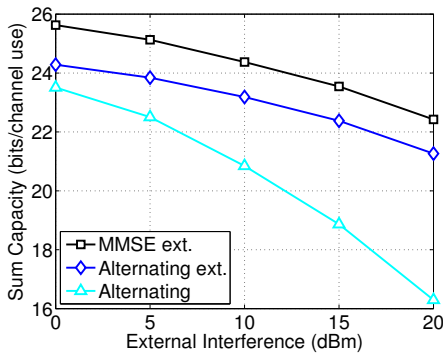
(c) SNR of 20 dB at the border of the cell.

(d) SNR of 30 dB at the border of the cell.

Figure 5.15 – Sum rate achieved by the algorithms versus external interference level for different SNR values at the border of the cell.

In Figure 5.15, the users were uniformly placed over all cells and we evaluated the behavior of the sum capacity achieved by each algorithm with external interference level variation for some SNR values. We can force the users to perceive a wide range of SINRs by varying the interference values within the range from 0 to 20 dBm, e.g., a user placed 300 m far from the cluster border can vary the SINR from -22 up to 26 dB for different SNRs.

We can verify, especially in low SNR cases, that there is a great impact of the external interference on the performance of the algorithms that do

not try to mitigate it. Moreover, we perceived that IA based algorithms perform reasonably well on mitigating external interference, since the achieved sum capacity decreases at a much slower pace, even for high values of external interference, in the available scenarios.

The maximum achievable DoF causes the perceived loss for high values of external interference with regard to the IA based algorithm. As stated before, this configuration allows to align only two interferers while these enhanced IA based algorithms try to adapt, as much as possible, the interference subspace to the external interference direction. Nevertheless, perfect alignment is almost surely not possible, which for severe external interference results in performance losses [9].

Now, we present figures varying the average SNR value at the cell border for different levels of external interference. Considering the users are distributed closer to the border of the cluster, there are few users that perceive high interference in this regular scenario, since most users are closer to the center of the cluster.

Figure 5.16, at the left side, presents sum capacity results of the scenario in which users are placed over all the cluster for cases with external interference at the border of the cluster of 0, 10 and 20 dBm. When users experience higher external interference, the enhanced IA algorithms perform better than the conventional ones. However, the IA does not necessarily need coordination. Moreover, the MMSE-based algorithm achieves higher sum capacity values than the alternating algorithm, as expected, since this last one uses a ZF-based approach.

Figure 5.16, at the right side, presents the sum capacity results for the scenario in which users are closer to the border. When the external interference is low, the curves have the same behavior as the previous results for the uniform distribution. However, as the external interference level increases, we can verify that the algorithms that deal with the external interference perform better.

Figure 5.17 shows the results related to the BER metric. We can evaluate that IA algorithms achieve the worst result, due to their incapability to mitigate the external interference. The use of enhanced algorithms that treat the interference provides a significant gain, especially for the MMSE-based algorithm, due to its design criterion, which tries to minimize the mean square error at the reception.
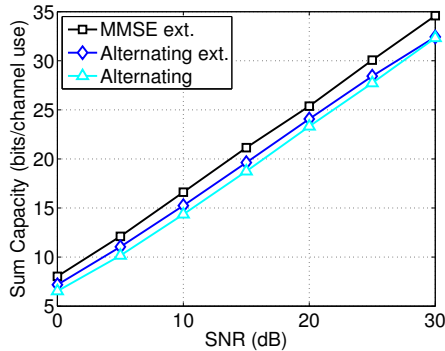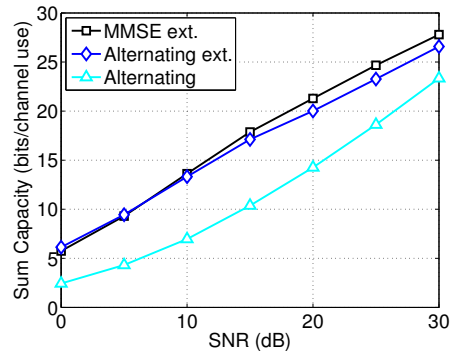
(a) External Interference of 0 dBm. Users distributed over all cells.
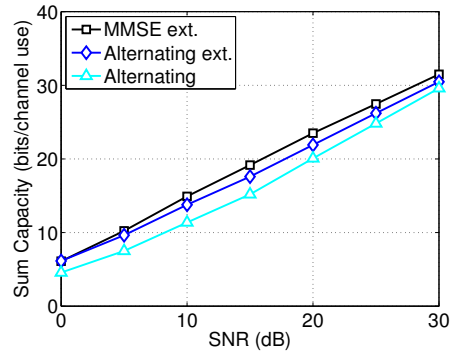
(b) External Interference of 0 dBm. Users after 2/3 of the cluster radius.
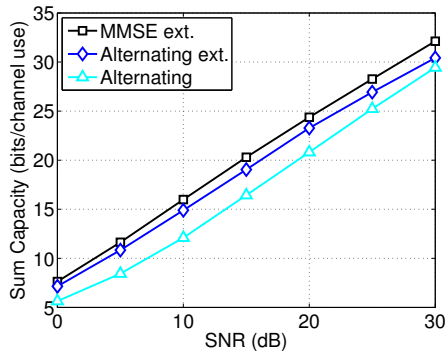
(c) External Interference of 10 dBm. Users distributed over all cells.

(d) External Interference of 10 dBm. Users after 2/3 of the cluster radius.

(e) External Interference of 20 dBm. Users distributed over all cells.

(f) External Interference of 20 dBm. Users after 2/3 of the cluster radius.

Figure 5.16 – Sum rate versus SNR for different external interference values at the border of the cluster. At the left side, the results relate to the case in which users are distributed over all cells and at the right side, users are distributed respecting a distance of 2/3 of the cluster radius.

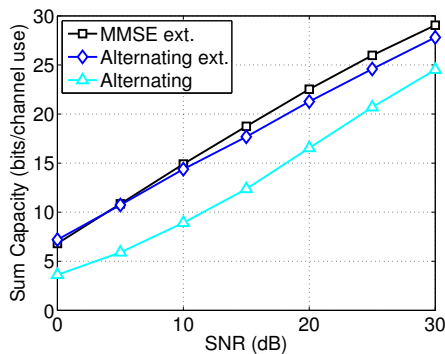(a) External Interference of 0 dBm.
Users distributed over all cells.

(b) External Interference of 0 dBm.
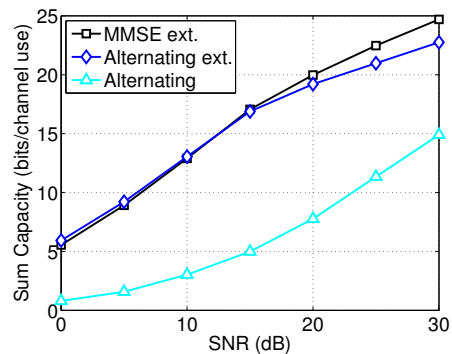Users after 2/3 of the cluster radius.
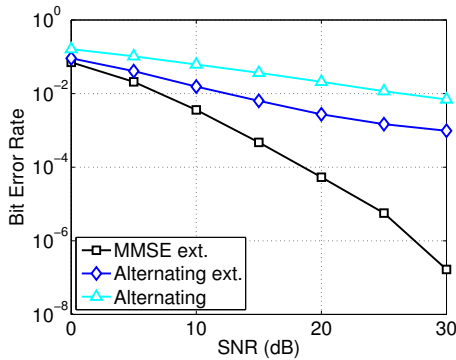
(c) External Interference of 10 dBm.
Users distributed over all cells.

(d) External Interference of 10 dBm.
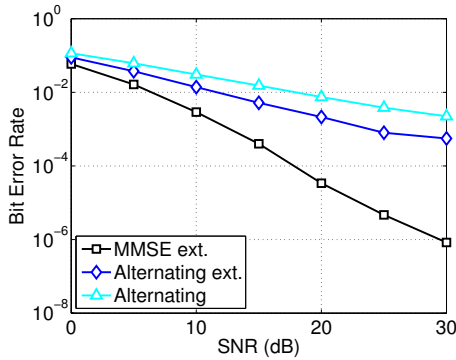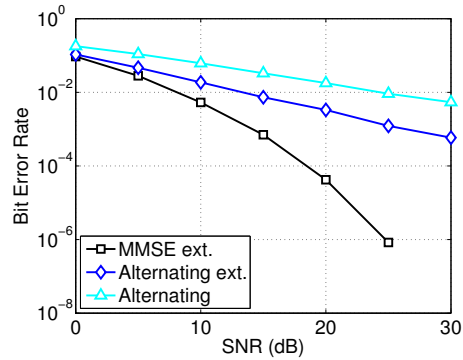Users after 2/3 of the cluster radius.
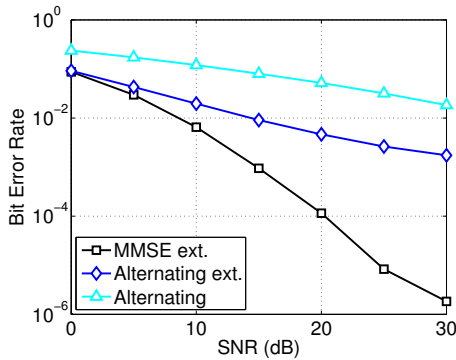
(e) External Interference of 20 dBm.
Users distributed over all cells.
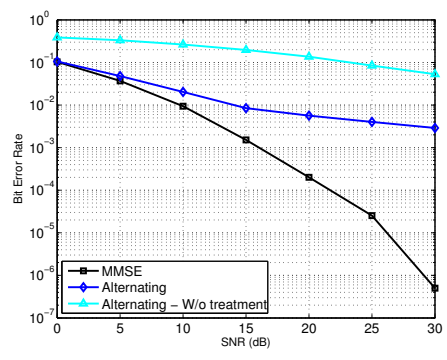
(f) External Interference of 20 dBm.
Users after 2/3 of the cluster radius.

Figure 5.17 – BER versus SNR for different external interference values at the border of the cluster. At the left side, the results relate to the case in which users are distributed over all cells and at the right side, users are distributed respecting a distance of 2/3 of the cluster radius.
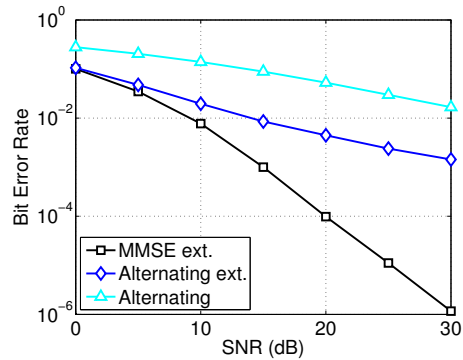
5.7 Remarks and Conclusions

In this chapter, we presented the simulation results obtained by means of Monte-Carlo simulations. Considering the perfect CSI, we have presented a comparative analysis of the rate utility and "α-fair" utility functions with the distributed pricing algorithm. We have empirically determined an interval of α values for the "α-fair" utility function that provides a higher sum rate than the rate utility.

Moreover, simulation results for scheduling strategies using the greedy algorithms showed that the Fubini-Study and chordal distances provide gains with regard to a random selection. Then, we examined the joint antenna and user selection scheme considering CSI.

Finally, applying the other IA algorithms, we analyzed the impact when antenna correlation, CSI or external interference are considered. As expected, all the IA algorithms suffered capacity losses because the behavior of IA algorithms is dependent on the channel quality. After that, we have evaluated the impact of the external interference on the performance of IA algorithms. The IA approach tries to align the internal interference in the direction of the external interference and they were evaluated in different scenarios.

Chapter 6

Conclusions and Perspectives

In this work, we present an overview, motivation and basic concepts about Interference Alignment (IA) including some upper bounds, feasibility conditions and channel knowledge feedback. We have focused our attention on signal alignment in interference networks with three nodes equipped with single or multiple antennas. We have taken into account both closed-form solutions of interference alignment, as well as distributed algorithms that permit to find the precoding matrices iteratively.

A common structure is shared among the different algorithms with the used metric being the main variation. Among the discussed algorithms, we contribute with the pricing algorithm. Several papers in the literature analyze the distributed pricing algorithm performance in different scenarios, as well as its convergence. However, none of them investigates the performance impact regarding the choice of the utility function. Therefore, we have presented a comparative analysis of the rate utility and "α-fair" utility functions with the distributed pricing algorithm. We have determined empirically an interval of α values for the "α-fair" utility function that provides a higher sum rate than the rate utility.

As any other technique, IA sum rate capacity is limited by the requirement of CSI at the transmitter. Hence, we have analyzed this practical consideration. The simulations show that all suggested methods are more sensitive to CSI error than antenna correlation. Moreover, satisfactory results are obtained because the IA approach tries to align the internal interference in the direction of the external interference. Finally, simulation results using the greedy algorithms showed that

the Fubini-Study and chordal distances provide gains with regard to a random selection.

The main contributions given by this work can be summarized as follows:

i. Comparative analysis of the rate utility and "α-fair" utility functions with the distributed pricing algorithm;

ii. We have evaluated the impact of transmit antenna correlation and CSI error and we analyze them in different scenarios;

iii. We have evaluated the impact of the external interference on the performance of IA algorithms;

iv. Different selection criteria using the greedy algorithms showed that the Fubini-Study and chordal distances provide gains with regard to a random selection;

v. We propose to use a joint antenna and user selection scheme for IA to find an appropriate metric which allows to increase the subspace distance for maximizing the capacity of the system.

As next steps we intend:

i. To investigate another definition of the interference price π_k (the more sensitive the utility of a user is to interference, the greater its interference price should be) because no derivation of an optimal price is available in the literature;

ii. To evaluate several scenarios to identify in which situations it is more favorable to use IA;

iii. To investigate the design of IA algorithms when the links of distant users can be disregarded, i.e., when the channel matrix has some near-zero values;

iv. In practical cellular systems to employ a finite set of precoders and this should be taken into account for the applicability of IA in practice;

v. To determine the number of necessary antennas and/or users for these considered metrics with interference alignment in mind;

vi. to investigate strategies for providing cooperative management of the resources of wireless networks through IA, relay, femtocells and D2D.

Bibliography

[1] G. J. Foschini and M. J. Gans, "On limits of wireless communications when using multiple antennas," *Wireless Pers. Commun.* **6**(3), pp. 311–335, 1998.

[2] Telatar, Emre, "Capacity of multi-antenna Gaussian channels," *European Transactions on Telecommunications* **10**, pp. 585–595, 1999.

[3] A. Ghasemi, A. S. Motahari, and A. K. Khandani, "Interference Alignment for the K User MIMO Interference Channel," *Arxiv preprint* **abs/0909.4**, p. 19, Sept. 2009.

[4] R. H. Etkin, D. Tse, and H. Wang, "Gaussian Interference Channel Capacity to Within One Bit," *IEEE Transactions on Information Theory* **54**, pp. 5534–5562, Dec. 2008.

[5] F. Miatton, *Interference alignment at intermediate SNR with perfect or noisy CSI.* PhD thesis, KTH, 2010.

[6] S. A. Jafar and S. Shamai, "Degrees of Freedom Region of the MIMO X Channel," *IEEE Transactions on Information Theory* **54**, pp. 151–170, Jan. 2008.

[7] C. M. Yetis, T. Gou, S. A. Jafar, and A. H. Kayran, "On Feasibility of Interference Alignment in MIMO Interference Networks," *IEEE Transactions on Signal Processing* **58**, pp. 4771–4782, Sept. 2010.

[8] K. Gomadam, V. R. Cadambe, and S. A. Jafar, "Approaching the Capacity of Wireless Networks through Distributed Interference Alignment," in *IEEE Global Telecommunications Conference*, pp. 1–6, IEEE, 2008.

[9] S. W. Peters and R. W. Heath, "Cooperative algorithms for MIMO interference channels," *IEEE Transactions on Vehicular Technology* **60**, pp. 206–218, Jan. 2011.

[10] S. A. Jafar, "Interference alignment: A new look at signal dimensions in a communication network.," *Foundations and Trends in Communications and Information Theory* **7**(1), pp. 1–136, 2011.

[11] M. Maddah-ali, A. S. Motahari, and A. K. Khandani, "Signaling over MIMO Multi-Base Systems: Combination of Multi-Access and Broadcast Schemes," in *IEEE International Symposium on Information Theory*, pp. 2104–2108, IEEE, July 2006.

[12] V. R. Cadambe and S. A. Jafar, "Interference Alignment and Degrees of Freedom of the K User Interference Channel," *IEEE Transactions on Information Theory* **54**, pp. 3425–3441, Aug. 2008.

[13] T. Gou and S. A. Jafar, "Degrees of Freedom of the K User $M \times N$ MIMO Interference Channel," *Arxiv preprint* **abs/0809.0099**, pp. 1–28, Aug. 2008.

[14] V. R. Cadambe and S. A. Jafar, "Degrees of freedom of wireless X networks," in *IEEE International Symposium on Information Theory*, pp. 1268–1272, IEEE, July 2008.

[15] C. Suh and D. Tse, "Interference Alignment for Cellular Networks," *46th Annual Allerton Conference on Communication, Control, and Computing* , pp. 1037–1044, Sept. 2008.

[16] J. Sun, Y. Liu, and G. Zhu, "On degrees of freedom of the cellular network," *Science China Information Sciences* **53**, pp. 1034–1043, Apr. 2010.

[17] Z. K. M. Ho and D. Gesbert, "Balancing Egoism and Altruism on the Interference Channel: The MIMO case," in *IEEE International Conference on Communications*, pp. 1–5, Jan. 2010.

[18] S. Gollakota, S. D. Perli, and D. Katabi, "Interference alignment and cancellation," *ACM SIGCOMM Computer Communication Review* **39**, p. 159, Aug. 2009.

[19] C. Shi, D. A. Schmidt, R. A. Berry, M. L. Honig, and W. Utschick, "Distributed Interference Pricing for the MIMO Interference Channel," *IEEE International Conference on Communications* , pp. 1–5, June 2009.

[20] Z. K. M. Ho and D. Gesbert, "Balancing Egoism and Altruism on the single beam MIMO Interference Channel," *IEEE Transactions on Signal Processing* **June**, pp. 1–20, 2010.

[21] J. Klotz and A. Sezgin, "Antenna selection criteria for interference alignment," in *IEEE 21st International Symposium on Personal Indoor and Mobile Radio Communications (PIMRC)*, pp. 527–531, Sep. 2010.

[22] J. H. Lee and W. Choi, "Interference alignment by opportunistic user selection in 3-user MIMO interference channels," in *IEEE International Conference on Communications (ICC)*, pp. 1–5, Jun. 2011.

[23] C. Huang, S. A. Jafar, and S. Shamai, "On degrees of freedom region of MIMO networks without CSIT," *Arxiv preprint arxiv:* , 2009.

[24] M. A. Maddah-Ali and D. Tse, "On the degrees of freedom of MISO broadcast channels with delayed feedback," Tech. Rep. UCB/EECS-2010-122, EECS Department, University of California, Berkeley, Sep 2010.

[25] N. Lee, J.-B. Lim, and J. Chun, "Degrees of Freedom of the MIMO Y Channel: Signal Space Alignment for Network Coding," *IEEE Transactions on Information Theory* **56**, pp. 3332–3342, July 2010.

[26] V. R. Cadambe and S. A. Jafar, "Degrees of Freedom of Wireless Networks With Relays, Feedback, Cooperation, and Full Duplex Operation," *IEEE Transactions on Information Theory* **55**, pp. 2334–2344, May 2009.

[27] H. Ning, C. Ling, and K. Leung, "Relay-aided interference alignment: Feasibility conditions and algorithm," in *IEEE International Symposium on Information Theory Proceedings (ISIT)*, pp. 390–394, June 2010.

[28] M. Guillaud and D. Gesbert, "Interference alignment in the partially connected K-user MIMO interference channel," in *Proc. European Signal Processing Conference (EUSIPCO), Barcelona, Spain*, pp. 1095–1099, Sept. 2011.

[29] M. Westreicher and M. Guillaud, "Interference alignment over partially connected interference networks: Application to the cellular case," in *IEEE Wireless Communications and Networking Conference (WCNC)*, pp. 647–651, Apr. 2012.

[30] B. Guler and A. Yener, "Interference alignment for cooperative MIMO femtocell networks," in *IEEE Global Telecommunications Conference (GLOBECOM)*, pp. 1–5, Dec. 2011.

[31] N. Lertwiram, P. Popovski, and K. Sakaguchi, "A study of trade-off between opportunistic resource allocation and interference alignment in femtocell scenarios," *IEEE Wireless Communications Letters* **PP**(99), pp. 1–4, 2012.

[32] G. Fodor, E. Dahlman, G. Mildh, S. Parkvall, N. Reider, G. Miklós, and Z. Turányi, "Design aspects of network assisted

device-to-device communications," *Communications Magazine, IEEE* **50**, pp. 170–177, Mar. 2012.

[33] H. E. Elkotby, K. M. F. Elsayed, and M. H. Ismail, "Exploiting interference alignment for sum rate enhancement in d2d-enabled cellular networks," in *IEEE Wireless Communications and Networking Conference (WCNC)*, pp. 1624–1629, Apr. 2012.

[34] D. Love and R. Heath, "Limited feedback unitary precoding for spatial multiplexing systems," *IEEE Transactions on Information Theory* **51**, pp. 2967–2976, Aug. 2005.

[35] H. G. Ghauch, *Interference alignment for multiuser cellular networks with multiantenna terminals.* PhD thesis, Carnegie Mellon University, 2011.

[36] H. Shen, B. Li, and Y. Luo, "Precoding design using interference alignment for the network MIMO," in *IEEE 20th International Symposium on Personal, Indoor and Mobile Radio Communications*, pp. 2519–2523, Sept. 2009.

[37] D. Tse and P. Viswanath, *Fundamentals of wireless communication*, Cambridge University Press, New York, NY, USA, 2005.

[38] E. Biglieri, R. Calderbank, A. Constantinides, A. Goldsmith, A. Paulraj, and H. V. Poor, *MIMO Wireless Communications*, Cambridge University Press, New York, NY, USA, 2007.

[39] H. Özcelik, N. Czink, and E. Bonek, "What makes a good MIMO channel model?," in *Proc. IEEE Vehicular Technology Conference (VTC)*, pp. 156–160, June 2005.

[40] B. N. Makouei, J. G. Andrews, and R. W. Heath, "MIMO Interference Alignment Over Correlated Channels With Imperfect CSI," *IEEE Transactions on Signal Processing* **59**, pp. 2783–2794, June 2011.

[41] TSG-RAN Working Group 4, "LTE channel models for concept evaluation in RAN1," Tech. Rep. R4-0.60101, 3GPP, February 2007.

[42] D. A. Schmidt, C. Shi, R. A. Berry, M. L. Honig, and W. Utschick, "Distributed Resource Allocation Schemes: Pricing Algorithms for Power Control and Beamformer Design in Interference Networks," *IEEE Signal Processing Magazine* **26**, pp. 53–63, Sept. 2009.

[43] S. A. Jafar and M. Fakhereddin, "Degrees of Freedom for the MIMO Interference Channel," *IEEE Transactions on Information Theory* **53**, pp. 2637–2642, July 2007.

[44] H. Ning, C. Ling, and K. K. Leung, "Feasibility condition for interference alignment with diversity," **57**(5), pp. 2902–2912, 2011.

[45] C. M. Yetis, T. Gou, S. A. Jafar, and A. H. Kayran, "On Feasibility of Interference Alignment in MIMO Interference Networks," *Arxiv preprint arXiv:0911.4507* , pp. 1–13, Nov. 2009.

[46] H. Sung, S. Park, K. Lee, and I. Lee, "Linear precoder designs for K-user interference channels," *IEEE Transactions on Wireless Communications* **9**, pp. 291–301, Jan. 2010.

[47] P. Mohapatra, K. Nissar, and C. Murthy, "Interference alignment algorithms for the K user constant MIMO interference channel," *Signal Processing, IEEE Transactions on* **59**, pp. 5499–5508, Nov 2011.

[48] H. Shen, B. Li, M. Tao, and Y. Luo, *The New Interference Alignment Scheme for the MIMO Interference Channel*, IEEE, Apr. 2010.

[49] C. Shi, R. A. Berry, and M. L. Honig, "Distributed interference pricing with MISO channels," in *Proc. 46th Annual Allerton Conference on Communication, Control, and Computing*, pp. 539 –546, Sep. 2008.

[50] C. Shi, R. A. Berry, and M. L. Honig, "Local interference pricing for distributed beamforming in MIMO networks," in *Proc. IEEE Military Communications Conference*, pp. 1–6, Oct. 2009.

[51] D. A. Schmidt, C. Shi, R. A. Berry, M. L. Honig, and W. Utschick, "Minimum Mean Squared Error interference alignment," in *Proc. 43rd Asilomar Conference on Signals, Systems and Computers*, pp. 1106–1110, Nov. 2009.

[52] J. Huang, R. A. Berry, and M. L. Honig, "Distributed interference compensation for wireless networks," *IEEE Journal on Selected Areas in Communications* **24**, pp. 1074 – 1084, May 2006.

[53] S. W. Peters and R. W. Heath, "Interference Alignment via Alternating Minimization," in *Proc. IEEE International Conference on Acoustics, Speech and Signal Processing (ICASSP)*, pp. 2445–2448, Apr. 2009.

[54] O. El Ayach, S. W. Peters, and R. W. Heath, "Real world feasibility of interference alignment using MIMO-OFDM channel measurements," in *Proc. IEEE Conference on Military Communications*, pp. 1–6, Oct. 2009.

[55] J. H. Conway, R. H. Hardin, and N. J. A. Sloane, "Packing lines, planes, etc.: Packings in Grassmannian space," *Experimental Mathematics* **5**, pp. 139–159, Jan. 1996.

[56] K. Schober, P. Janis, and R. Wichman, "Geodesical codebook design for precoded MIMO systems," *IEEE Communications Letters* **13**, pp. 773–775, Oct. 2009.

[57] B. Zhou, B. Bai, Y. Li, D. Gu, and Y. Luo, "Chordal distance-based user selection algorithm for the multiuser MIMO downlink with perfect or partial CSIT," in *IEEE International Conference on Advanced Information Networking and Applications (AINA)*, pp. 77–82, Mar. 2011.

[58] Z. Shen, R. Chen, J. Andrews, R. Heath, and B. Evans, "Low complexity user selection algorithms for multiuser MIMO systems with block diagonalization," in *Thirty-Ninth Asilomar Conference on Signals, Systems and Computers*, pp. 628–632, Nov. 2005.

[59] S. Kaviani and W. Krzymien, "User selection for multiple-antenna broadcast channel with zero-forcing beamforming," in *IEEE Global Telecommunications Conference (GLOBECOM)*, pp. 1–5, Dec. 2008.